91-11-325

IU/NTC 91-12
CEBAF-PR-91-037

RELATIVISTIC NUCLEAR MANY-BODY THEORY*

Brian D. Serot

Physics Department and Nuclear Theory Center
Indiana University
Bloomington, IN 47405

John Dirk Walecka

Continuous Electron Beam Accelerator Facility
12000 Jefferson Avenue
Newport News, VA 23606

September 11, 1991

ABSTRACT

Nonrelativistic models of nuclear systems have provided important insight into nuclear physics. In future experiments, nuclear systems will be examined under extreme conditions of density and temperature, and their response will be probed at momentum and energy transfers larger than the nucleon mass. It is therefore essential to develop reliable models that go beyond the traditional nonrelativistic many-body framework. General properties of physics, such as quantum mechanics, Lorentz covariance, and microscopic causality, motivate the use of quantum field theories to describe the interacting, relativistic, nuclear many-body system. Renormalizable models based on hadronic degrees of freedom (*quantum hadrodynamics*) are presented, and the assumptions underlying this framework are discussed. Some applications and successes of quantum hadrodynamics are described, with an emphasis on the new features arising from relativity. Examples include the nuclear equation of state, the shell model, nucleon–nucleus scattering, and the inclusion of zero-point vacuum corrections. Current issues and problems are also considered, such as the construction of improved approximations, the full role of the quantum vacuum, and the relationship between quantum hadrodynamics and quantum chromodynamics. We also speculate on future developments.

*Invited talks given at the Seventh International Conference on Recent Progress in Many-Body Theories, Minneapolis, MN, August 26–31, 1991.

The study of atomic nuclei plays an important role in the development of many-body theories. Since early experimental probes of the nucleus were limited to energy scales considerably less than the nucleon mass $M \approx 939\,\mathrm{MeV}/c^2$, the nucleus was initially described as a collection of nonrelativistic nucleons interacting through an instantaneous two-body potential, with the dynamics given by the Schrödinger equation. In this approach, the two-body potential is fit to the empirical properties of the deuteron and low-energy nucleon–nucleon (NN) scattering, and one then attempts to predict the properties of many-nucleon systems. This is a difficult problem, because the NN potential is strong, short-ranged ($R \approx 1\,\mathrm{fm}$), and has a very repulsive central core. Nevertheless, over a period of many years and with the advent of more and more powerful computers, reliable methods have been developed for solving the nonrelativistic nuclear many-body problem. At present, essentially exact solutions exist for both the three-nucleon system and for "nuclear matter," the hypothetical uniform system with equal numbers of neutrons and protons ($N = Z$) obtained by turning off the Coulomb potential and letting the total number of baryons $B = N + Z$ go to infinity. Similar results for up to 8 (and possibly 16) nucleons should be obtained in the near future.

On balance, these microscopic nonrelativistic calculations are reasonably successful. With modern NN potentials, the ^{3}He system is underbound by $\approx 0.8\,\mathrm{MeV}$ (about 10%),[1] and the calculated rms charge radius is $\approx 9\%$ too large. The predicted energy/nucleon of nuclear matter at equilibrium is close to the empirical value

$$(E/B) - M \approx -16\,\mathrm{MeV}\,, \tag{1}$$

but the saturation density, which is related to the Fermi wavenumber k_F through $\rho_\mathrm{B} = B/V = 2k_\mathrm{F}^3/3\pi^2$, is too high, as the calculated value is $k_\mathrm{F} \approx 1.5\,\mathrm{fm}^{-1}$, while the empirical result is $k_\mathrm{F} \approx 1.3\,\mathrm{fm}^{-1}$. In addition, some general features of nuclear structure are qualitatively understood, for example, the importance of the Pauli principle in reducing NN correlations, which justifies both the shell model and the single-nucleon optical potential, and the interplay of single-particle and collective degrees of freedom, which determines the shape of the nucleus. By adding a small, phenomenological, density-dependent interaction to the free NN potential, one can quantitatively reproduce the single-particle structure and charge and mass densities of a large number of nuclei.[2] Furthermore, by using nuclear current operators constructed from the properties of free nucleons, an accurate picture of weak and electromagnetic interactions in nuclei has emerged. These successful results have stimulated the development of a diverse array of nuclear models that can be applied to nuclear structure and reactions throughout the periodic table.[3]

In spite of these successes, there are important reasons for developing a relativistic description of nuclear systems. For example, the properties of neutron stars depend on the neutron matter equation of state at densities up to an order of magnitude higher than those observed in ordinary nuclei; nucleon velocities are certainly relativistic at these densities. In addition, although the empirical low-energy NN scattering amplitude

has conventionally been parametrized using Galilean invariants, a decomposition using Lorentz invariants reveals surprising new features. In particular, the empirical Lorentz scalar, vector, and pseudoscalar amplitudes are much larger than the amplitudes deduced from the nonrelativistic decomposition. These large amplitudes have important consequences for the spin-, velocity-, and density-dependence of the NN interaction and are at the heart of recent relativistic descriptions of nucleon–nucleus scattering that reproduce spin observables in a very economical fashion.[4–6]

Furthermore, medium-energy accelerators that probe nuclei at distance scales less than 1 fm reveal that the conventional framework is inadequate for a complete understanding of ordinary nuclei. For example, experiments on the electrodisintegration of the deuteron show unambiguously the presence of pion-exchange currents, which arise when the incoming (virtual) photon couples to a pion being exchanged between two nucleons. In addition, medium-energy pion–nucleus and proton–nucleus scattering indicate the importance of baryon resonances, such as the $\Delta(1232)$, in nuclear reactions. Thus both the dynamical nature of the NN interaction and the structure of the nucleon itself become important at an energy scale of several hundred MeV. As supporting evidence for this new dynamics, accurate microscopic meson-exchange models have been constructed to describe the NN interaction. These contain several mesons, the most important of which are the $\pi(0^-,1)$, $\sigma(0^+,0)$, $\omega(1^-,0)$, and $\rho(1^-,1)$, where the indicated quantum numbers denote spin, parity, and isospin, together with both N and Δ degrees of freedom. These meson-exchange models reproduce the large Lorentz-invariant scattering amplitudes mentioned earlier. Nevertheless, if one adheres to a nonrelativistic many-body description of nuclear structure, the new dynamical features can be incorporated into the conventional framework only by reducing them to an approximate form that is appropriate for the Schrödinger equation.

In future experiments, a new generation of accelerators will allow us to study nuclei at higher energies, at shorter distances, and with greater precision than ever before. For example, proton–nucleus collisions will provide complete spin information on both the projectile and the target, electron–nucleus scattering will sample distance scales down to tenths of a Fermi, and ultra-relativistic heavy ion collisions may produce nuclear densities of 10 times equilibrium density at temperatures of 100 to 200 MeV. These experiments will clearly involve physics that goes far beyond the Schrödinger equation, such as relativistic motion of the nucleons, dynamical meson exchanges and baryon resonances, modifications of hadron structure in the nucleus, and the dynamics of the quantum vacuum, which may include the production of a quark-gluon plasma. The challenge to theorists is to develop techniques that describe this new physics, while maintaining the important general properties of quantum mechanics, covariance, electromagnetic gauge invariance, and microscopic causality.

Since quantum chromodynamics (QCD) of quarks and gluons appears to be the fundamental theory of the strong interaction, it is natural to look to QCD as the means to describe this new physics. While this may be desirable in principle, there are many difficulties in practice, primarily because the QCD coupling is strong at distance scales relevant for the vast majority of nuclear phenomena. Although significant progress has

been made in the last 10 years in performing strong-coupling lattice calculations, actual QCD predictions at nuclear length scales with the precision of existing (and anticipated) data are not presently available. This situation will probably persist for some time, particularly with regard to many-nucleon systems. Even if it becomes possible to use QCD to describe many-nucleon systems, this description is likely to be awkward, since quarks cluster into hadrons at low energies, and hadrons (not quarks or gluons) are the degrees of freedom actually observed in experiments.

In contrast, a description based on hadronic degrees of freedom is attractive for several reasons. First, these variables are the most efficient at normal densities and low temperatures, and for describing particle absorption and emission. Moreover, hadronic calculations can be calibrated by requiring that they reproduce empirical nuclear properties and scattering amplitudes; we can then extrapolate to the extreme situations mentioned earlier. Finally, although hadronic models must ultimately fail when the quark and gluon dynamics becomes essential, we must understand the limitations of hadronic models to isolate and identify true signatures of subhadronic dynamics.

Our basic goal is therefore to formulate a consistent microscopic treatment of nuclear systems using hadronic (baryon and meson) degrees of freedom. Since the physical phenomena of interest are relativistic and involve particle production and absorption, the only known consistent framework for their description is relativistic quantum field theory based on a local, Lorentz-invariant lagrangian density. We will refer to these hadronic relativistic field theories as *quantum hadrodynamics*, or QHD.[7] QHD is consistent in the same sense as any other relativistic quantum field theory: the assumptions about the relevant degrees of freedom, the form of the lagrangian, and the empirical data that determine the parameters are made at the outset, and one then attempts to extract concrete predictions from the implied formalism. In principle, these assumptions permit the formulation of "conserving approximations"[8,9] that maintain the important general properties mentioned above. Calculations can then be compared to the data to decide where QHD succeeds and where it fails.

We emphasize, however, that QHD still contains strong couplings, as does any treatment of the nuclear many-body problem. It is therefore necessary to develop reliable nonperturbative approximations, so that unambiguous comparisons between theory and experiment can be made. The formulation of practical, reliable techniques for finite-density calculations in strong-coupling relativistic quantum field theories is basically an unsolved problem.[10–12] The development of such tools in a hadronic field theory is not only useful in its own right, but it may also provide insight into similar approaches for QCD. Nuclear many-body theory has had such influence in other areas of physics in the past.

We shall also require that QHD be a renormalizable theory. This means that any QHD model can be characterized by a finite number of coupling constants and masses.[13,14] Thus the model is self-contained, and calculations can be carried out beyond the "tree level" without introducing additional parameters (such as vertex cutoffs) determined solely by short-distance phenomena. This minimizes the sensitivity of cal-

culated results to short-distance input. The dynamical assumption underlying renormalizability is that the quantum vacuum and the internal structure of the hadrons can be described in terms of hadronic degrees of freedom alone. This assumption must ultimately break down, since at very short distances, hadrons are composed of quarks and gluons. For QHD to be useful, nuclear observables of interest must not be dominated by contributions from short distances, where QHD is inappropriate. This conjecture must be tested, and its limitations uncovered, by performing detailed calculations in a consistent relativistic framework.

There are alternative methods for describing hadronic and nuclear systems that go beyond the Schrödinger equation. Several meson-exchange models of the NN interaction have been developed and applied to nuclear systems, both relativistically and nonrelativistically.[15–17] These models focus primarily on the precise reproduction of the two-nucleon data, and they contain many mesonic degrees of freedom and adjustable parameters. These models are not renormalizable, and the number of parameters and the form of the interactions are unconstrained, except by the desire to reproduce the data. Typically, the treatment of the quantum vacuum is either incomplete or neglected entirely,[18] making it impossible to formulate conserving approximations. These features make it difficult to distinguish between hadronic dynamics and dynamics that arises from the underlying QCD degrees of freedom.

For these reasons, we will base our analysis on QHD as defined above, which presumably provides the correct description of many-baryon systems at large distances. Renormalizability restricts the form of the QHD lagrangian and the number of parameters. In a sense, renormalizable QHD is a means of defining a *purely* hadronic theory. By considering only a few hadronic degrees of freedom, we can study the role of meson dynamics and relativity in nuclear systems as simply as possible. Moreover, we have a self-contained model for studying the formal aspects of the relativistic many-body problem with strong couplings. Nevertheless, QHD becomes increasingly complicated at short distances, where a hadronic description must ultimately break down. Hopefully, the general features discussed below will remain valid even if the constraint of renormalizability at the hadronic level turns out to be too restrictive.

Due to limited space, this paper deals with only a fraction of the areas of current interest in QHD. We focus first on the simple model QHD–I,[19] which contains neutrons, protons, and the isoscalar, Lorentz scalar and vector mesons σ and ω. The development is based on the relativistic mean-field and Hartree approximations, and their application to both infinite nuclear matter and the ground states of atomic nuclei. We discuss some successes of this model, including the nuclear equation of state, the shell model, nucleon–nucleus scattering, and the addition of zero-point vacuum corrections. We concentrate on the new features that arise in a relativistic framework and emphasize the important concepts of Lorentz covariance and self-consistency. In the second half of this work, we consider QHD–II,[20,21] the extension of QHD–I to include isovector π and ρ mesons. QHD–II is based on the so-called linear σ model,[22–24] which contains neutrons, protons, pions, and neutral scalar mesons interacting in a chirally invariant fashion. We also discuss extensions beyond the relativistic mean-field and Hartree approximations, as

a means for constructing reliable calculational schemes, as well as recent efforts to incorporate the full role of the quantum vacuum and relativistic pion dynamics in a consistent fashion. At the end, we return to consider the relationship between QHD and QCD and to speculate on future developments.

The reader is assumed to have a working knowledge of relativistic quantum field theory, canonical quantization, and the use of path integrals at zero temperature. For general background on relativistic field theory, the reader can turn to any of a number of texts;[25-30] a recent review exists for background on quantum hadrodynamics.[7]

ACCOMPLISHMENTS

A Simple Model

Quantum hadrodynamics as defined above is a general framework for the relativistic nuclear many-body problem. The detailed dynamics must be specified by choosing a particular renormalizable lagrangian density. To illustrate the relativistic formalism as simply as possible, we consider a model called QHD-I, which contains fields for baryons $\left[\psi = \begin{pmatrix} \psi_p \\ \psi_n \end{pmatrix}\right]$ and neutral scalar (ϕ) and vector (V^μ) mesons.[19]

The lagrangian density for this model is given by[7] ($\hbar = c = 1$)

$$\mathcal{L} = \overline{\psi}\left[\gamma_\mu(i\partial^\mu - g_v V^\mu) - (M - g_s\phi)\right]\psi + \tfrac{1}{2}(\partial_\mu\phi\partial^\mu\phi - m_s^2\phi^2) - \tfrac{1}{4}F_{\mu\nu}F^{\mu\nu} + \tfrac{1}{2}m_v^2 V_\mu V^\mu + \delta\mathcal{L}\,, \tag{2}$$

where $F^{\mu\nu} = \partial^\mu V^\nu - \partial^\nu V^\mu$ and $\delta\mathcal{L}$ contains counterterms. The parameters M, g_s, g_v, m_s, and m_v are phenomenological constants that may be determined (in principle) from experimental measurements. This lagrangian resembles massive QED with an additional scalar interaction, so the resulting relativistic quantum field theory is *renormalizable*.[31] The counterterms in $\delta\mathcal{L}$ are used for renormalization.

The motivation for this model has evolved considerably since it was introduced. As discussed in the Introduction, when the empirical nucleon–nucleon (NN) scattering amplitude is described in a Lorentz-covariant fashion, it contains strong isoscalar scalar and four-vector pieces,[4-6] and the simplest way to reproduce these pieces is through the exchange of neutral scalar and vector mesons. The neutral scalar and vector components are the most important for describing bulk nuclear properties, which is our main concern here. Other Lorentz components of the NN interaction, in particular the terms arising from pion exchange, average essentially to zero in spin-saturated nuclear matter and may be incorporated as refinements to the present model. The important point is that even in more refined models, the dynamics generated by scalar and vector mesons will remain; thus it is important to first understand the consequences of these degrees of freedom for relativistic descriptions of nuclear systems.

The field equations for this model follow from the Euler–Lagrange equations and

can be written as

$$(\partial_\mu \partial^\mu + m_s^2)\phi = g_s \overline{\psi}\psi \,, \tag{3}$$

$$\partial_\nu F^{\nu\mu} + m_v^2 V^\mu = g_v \overline{\psi}\gamma^\mu \psi \,, \tag{4}$$

$$[\gamma^\mu (i\partial_\mu - g_v V_\mu) - (M - g_s \phi)]\psi = 0 \,. \tag{5}$$

(The counterterms have been suppressed.) Equation (3) is simply the Klein–Gordon equation with a scalar source. Equation (4) looks like massive QED with the conserved baryon current

$$B^\mu \equiv (\rho_B, \boldsymbol{\mathcal{B}}) = \overline{\psi}\gamma^\mu \psi \,, \qquad \partial_\mu B^\mu = 0 \tag{6}$$

rather than the (conserved) electromagnetic current as source. Finally, eq. (5) is the Dirac equation with scalar and vector fields introduced in a minimal fashion. These field equations imply that the canonical energy-momentum tensor $T^{\mu\nu}$ is conserved ($\partial_\mu T^{\mu\nu} = \partial_\nu T^{\mu\nu} = 0$).

When quantized, eqs. (3)–(5) become *nonlinear quantum field equations*, whose exact solutions are very complicated. In particular, they describe mesons and baryons *that are not point particles*, but rather objects with intrinsic structure due to the implied (virtual) meson and baryon-antibaryon loops. It is here that the dynamical input of renormalizability is apparent, since we are assuming that this intrinsic structure (or at least the long-range part of it) can be described using hadronic degrees of freedom. The validity of this input and its limitations have yet to be tested consistently within the framework of QHD, and we will return to this question later.

We also expect the coupling constants in eqs. (3)–(5) to be large, so perturbative solutions are not useful. Fortunately, there is an approximate nonperturbative solution that should become increasingly valid as the nuclear density increases. Consider a system of B baryons in a large box of volume V at zero temperature. Assume that we are in the rest frame of the matter, so that the baryon flux $\boldsymbol{\mathcal{B}} = 0$. As the baryon density B/V increases, so do the source terms on the right-hand sides of eqs. (3) and (4). When the sources are large, the meson field operators can be replaced by their expectation values, which are classical fields:

$$\phi \to \langle \phi \rangle \equiv \phi_0 \,, \qquad V^\mu \to \langle V^\mu \rangle \equiv (V_0, \mathbf{0}) \,. \tag{7}$$

For our stationary, uniform system, ϕ_0 and V_0 are *constants* that are independent of space and time, and since the matter is at rest, the classical three-vector field $\mathbf{V} = 0$.

We emphasize the strategy involved in the preceding "mean-field" approximation. First, the resulting mean-field theory (MFT) should give the correct solution to the field equations in the high-density limit. More importantly, however, the MFT serves as a starting point for calculating corrections within the framework of QHD, using Feynman diagrams, path-integral methods, and so forth, as we will discuss later in this work.

When the meson fields in eq. (2) are approximated by the constant classical fields of eq. (7), we arrive at the mean-field lagrangian density

$$\mathcal{L}_{\rm MFT} = \overline{\psi}[i\gamma^\mu\partial_\mu - g_{\rm v}V_0\gamma_0 - (M - g_{\rm s}\phi_0)]\psi - \tfrac{1}{2}m_{\rm s}^2\phi_0^2 + \tfrac{1}{2}m_{\rm v}^2V_0^2\,. \tag{8}$$

(The counterterms have been suppressed.) The conserved baryon four-current remains as in eq. (6), and the canonical energy-momentum tensor becomes

$$T^{\mu\nu}_{\rm MFT} = i\overline{\psi}\gamma^\mu\partial^\nu\psi - \tfrac{1}{2}(m_{\rm v}^2V_0^2 - m_{\rm s}^2\phi_0^2)g^{\mu\nu}\,. \tag{9}$$

As discussed by Freedman,[32] there is no need to symmetrize $T^{\mu\nu}$ if we consider only uniform nuclear matter.

Since the meson fields are classical, only the fermion field must be quantized. The Dirac field equation follows from $\mathcal{L}_{\rm MFT}$:

$$[i\gamma_\mu\partial^\mu - g_{\rm v}\gamma_0V_0 - (M - g_{\rm s}\phi_0)]\psi(t,\mathbf{x}) = 0\,, \tag{10}$$

and since this equation is linear, it can be solved exactly. Note that the scalar field ϕ_0 shifts the baryon mass from M to $M^* \equiv M - g_{\rm s}\phi_0$, while the vector field V_0 shifts the energy spectrum. We look for normal-mode solutions with both positive and negative energies, as is natural for the Dirac equation. These solutions can be used to define quantum field operators ψ and $\psi^\dagger$ in the usual fashion, and by imposing the familiar equal-time anticommutation relations, we can construct the baryon number operator $\hat{B} \equiv \int \mathrm{d}^3x\,\overline{\psi}\gamma^0\psi$ and the four-momentum operators $\hat{P}^\mu = (\hat{H},\hat{\mathbf{P}}) \equiv \int \mathrm{d}^3x\,\hat{T}^{0\mu}$, with the results

$$\hat{H} - \langle 0|\hat{H}|0\rangle = \hat{H}_{\rm MFT} + \delta H\,, \tag{11}$$

$$\hat{H}_{\rm MFT} = \sum_{\mathbf{k}\lambda}(\mathbf{k}^2 + M^{*2})^{1/2}(A^\dagger_{\mathbf{k}\lambda}A_{\mathbf{k}\lambda} + B^\dagger_{\mathbf{k}\lambda}B_{\mathbf{k}\lambda}) + g_{\rm v}V_0\hat{B} + \tfrac{1}{2}(m_{\rm s}^2\phi_0^2 - m_{\rm v}^2V_0^2)V\,, \tag{12}$$

$$\delta H = -\sum_{\mathbf{k}\lambda}\left[(\mathbf{k}^2 + M^{*2})^{1/2} - (\mathbf{k}^2 + M^2)^{1/2}\right], \tag{13}$$

$$\hat{B} = \sum_{\mathbf{k}\lambda}(A^\dagger_{\mathbf{k}\lambda}A_{\mathbf{k}\lambda} - B^\dagger_{\mathbf{k}\lambda}B_{\mathbf{k}\lambda})\,, \tag{14}$$

$$\hat{\mathbf{P}} = \sum_{\mathbf{k}\lambda}\mathbf{k}\,(A^\dagger_{\mathbf{k}\lambda}A_{\mathbf{k}\lambda} + B^\dagger_{\mathbf{k}\lambda}B_{\mathbf{k}\lambda})\,. \tag{15}$$

Here the index λ denotes both spin and isospin projections. The quantities $A^\dagger_{\mathbf{k}\lambda}$, $B^\dagger_{\mathbf{k}\lambda}$, $A_{\mathbf{k}\lambda}$, and $B_{\mathbf{k}\lambda}$ appearing in these expressions are creation and destruction operators for (quasi)baryons and (quasi)antibaryons with shifted mass and energy, and $\hat{B}$ is the baryon number operator, which clearly counts the number of baryons minus the number of antibaryons. The correction term δH arises from placing the operators in $\hat{H}_{\rm MFT}$ in "normal order" and represents the contribution to the energy from the filled Dirac sea, where the baryon mass has been shifted by the uniform scalar field ϕ_0.[7] We will return

later to discuss this "zero-point energy" correction; for now let us concentrate on the MFT hamiltonian defined by eq. (12).

Since $\hat{H}_{\rm MFT}$ is diagonal, this model mean-field problem has been solved *exactly* once the meson fields are specified; their determination is discussed below. The solution retains the essential features of QHD: relativistic covariance, explicit meson degrees of freedom, and the incorporation of antiparticles. Furthermore, it yields a simple solution to the field equations that should become increasingly valid as the baryon density increases. Since $\hat{B}$ and $\hat{\mathbf{P}}$ are also diagonal, the baryon number and total momentum are constants of the motion, as are their corresponding densities $\rho_{\rm B}$ and $\mathcal{P}$, since the volume is fixed.

For uniform nuclear matter, the ground state is obtained by filling energy levels with spin-isospin degeneracy γ up to the Fermi momentum $k_{\rm F}$. (The generalization to finite temperature will be discussed at the end of this section.) The Fermi momentum is related to the baryon density by

$$\rho_{\rm B} = \frac{\gamma}{(2\pi)^3}\int_0^{k_{\rm F}} {\rm d}^3k = \frac{\gamma}{6\pi^2}\,k_{\rm F}^3\,, \tag{16}$$

where the degeneracy factor γ is 4 for symmetric ($N = Z$) matter and 2 for pure neutron matter ($Z = 0$). The constant vector field V_0 can be expressed in terms of conserved quantities from the expectation value of the vector meson field equation (4):

$$V_0 = \frac{g_{\rm v}}{m_{\rm v}^2}\rho_{\rm B}\,. \tag{17}$$

The expressions for the energy density and pressure now take the simple forms[7]

$$\mathcal{E} = \frac{g_{\rm v}^2}{2m_{\rm v}^2}\,\rho_{\rm B}^2 + \frac{m_{\rm s}^2}{2g_{\rm s}^2}\,(M - M^*)^2 + \frac{\gamma}{(2\pi)^3}\int_0^{k_{\rm F}} {\rm d}^3k\; E^*(k)\,, \tag{18}$$

$$p = \frac{g_{\rm v}^2}{2m_{\rm v}^2}\,\rho_{\rm B}^2 - \frac{m_{\rm s}^2}{2g_{\rm s}^2}\,(M - M^*)^2 + \frac{1}{3}\,\frac{\gamma}{(2\pi)^3}\int_0^{k_{\rm F}} {\rm d}^3k\;\frac{\mathbf{k}^2}{E^*(k)}\,, \tag{19}$$

where $E^*(k) \equiv (\mathbf{k}^2 + M^{*2})^{1/2}$. The first two terms in eqs. (18) and (19) arise from the classical meson fields. The final terms in these equations are those of a relativistic gas of baryons of mass M^*. These expressions give the nuclear matter equation of state at zero temperature in parametric form: $\mathcal{E}(\rho_{\rm B})$ and $p(\rho_{\rm B})$.

The constant scalar field ϕ_0, or equivalently the effective mass M^*, can be determined thermodynamically at the end of the calculation by minimizing $\mathcal{E}(M^*)$ with respect to M^*. This produces the *self-consistency condition*

$$\begin{aligned} M^* &= M - \frac{g_{\rm s}^2}{m_{\rm s}^2}\,\frac{\gamma}{(2\pi)^3}\int_0^{k_{\rm F}} {\rm d}^3k\;\frac{M^*}{E^*(k)} \\ &= M - \frac{g_{\rm s}^2}{m_{\rm s}^2}\,\langle :\overline{\psi}\psi: \rangle \equiv M - \frac{g_{\rm s}^2}{m_{\rm s}^2}\,\rho_{\rm s}\,, \end{aligned} \tag{20}$$

which also defines the scalar density $\rho_{\rm s}$. Equation (20) is equivalent to the MFT scalar field equation for ϕ_0. Note that the scalar density is smaller than the baryon density

[eq. (16)] due to the factor $M^*/E^*(k)$, which is an effect of Lorentz contraction. Thus the contribution of rapidly moving baryons to the scalar source is significantly reduced. Most importantly, eq. (20) is a *transcendental self-consistency equation* for M^* that must be solved at each value of k_F. This illustrates the *nonperturbative* nature of the mean-field solution.

An examination of the analytic expression (18) for the energy density shows that the system is unbound ($\mathcal{E}/\rho_B > M$) at either very low or very high densities.[19] At intermediate densities, the attractive scalar interaction will dominate if the coupling constants are chosen properly. The system then *saturates*. Nuclear matter with an equilibrium Fermi wavenumber $k_F^0 = 1.30$ fm^{-1} and an energy/nucleon $(\mathcal{E}/\rho_B - M) = -15.75$ MeV is obtained if the couplings are chosen as[(b)]

$$C_s^2 \equiv g_s^2\left(\frac{M^2}{m_s^2}\right) = 357.4\,, \qquad C_v^2 \equiv g_v^2\left(\frac{M^2}{m_v^2}\right) = 273.8\,. \tag{21}$$

The nuclear compressibility in this approximation is 545 MeV. Note that only the *ratios* of coupling constants to meson masses enter in eqs. (18), (19), and (20). The resulting saturation curve is shown in fig. 1. In this approximation, the relativistic properties of the scalar and vector fields are responsible for saturation; a Hartree–Fock variational estimate built on the nonrelativistic (Yukawa) potential limit of the interaction shows that such a system is unstable against collapse.

The solution of the self-consistency condition (20) for M^* yields an effective mass that is a decreasing function of the density, as illustrated in fig. 2. Evidently, M^*/M becomes small at high density and is significantly less than unity at ordinary nuclear densities. This is a consequence of the large scalar field $g_s\phi_0$, which is approximately 400 MeV and which produces a large attractive contribution to the energy/baryon. There is also a large repulsive energy/baryon from the vector field $g_v V_0 \approx 350$ MeV. Thus *the Lorentz structure of the interaction leads to a new energy scale in the problem*, and the small nuclear binding energy (≈ 16 MeV) arises from the cancellation between the large scalar attraction and vector repulsion. As the nuclear density increases, the scalar source ρ_s becomes small relative to the vector source ρ_B, and the attractive forces saturate, producing the minimum in the binding curve. Clearly, because of the sensitive cancellation involved near the equilibrium density, corrections to the MFT must be calculated before the importance of this new saturation mechanism can be assessed. Nevertheless, the Lorentz structure of the interaction provides an *additional saturation mechanism that is not present in the nonrelativistic potential limit*, as this limit ignores the distinction between ρ_s and ρ_B.

The corresponding curves for neutron matter obtained by setting $\gamma = 2$ are also shown in figs. 1 and 2, and the equation of state (pressure *vs.* energy density) for neutron matter at all densities is given in fig. 3. In this mean-field model, there is a van der Waals (liquid–gas) phase transition, and the properties of the two phases are deduced through a Maxwell construction. At high densities, the system approaches the

[(b)]The values $C_s^2 = 267.1$ and $C_v^2 = 195.9$ used in ref. 7 yield $k_F^0 = 1.42$ fm^{-1}. This is set L1 in table 1 below.

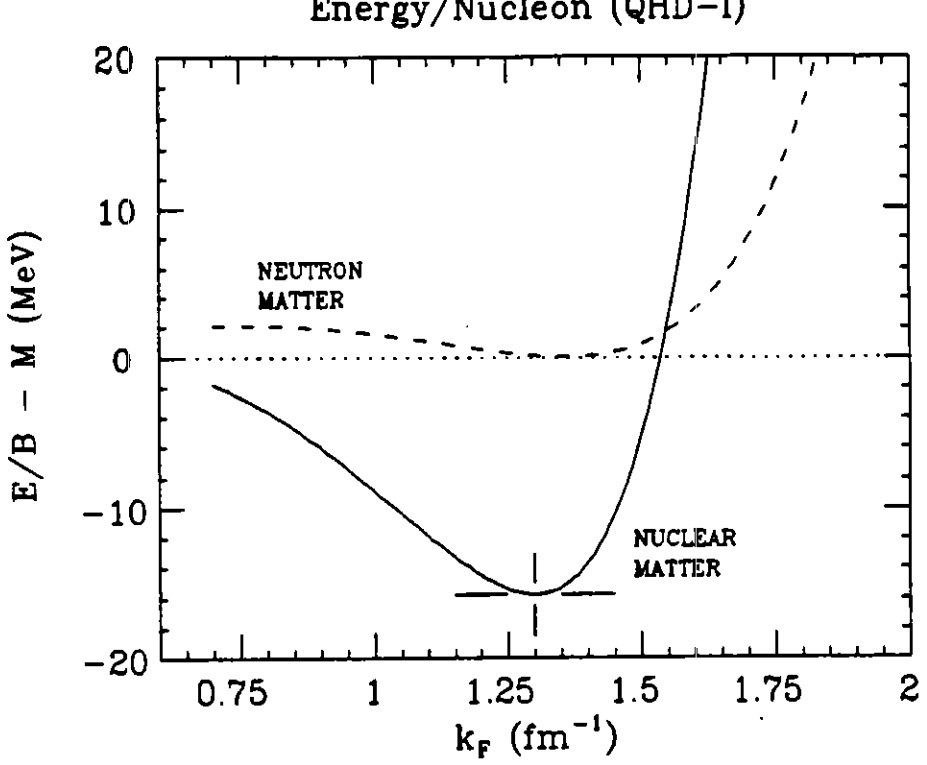

Figure 1: Saturation curve for nuclear matter. These results are calculated in the relativistic mean-field theory with baryons and neutral scalar and vector mesons (QHD-I). The coupling constants are chosen to fit the value and position of the minimum and are given in row L2 of table 1. The prediction for neutron matter ($\gamma = 2$) is also shown.

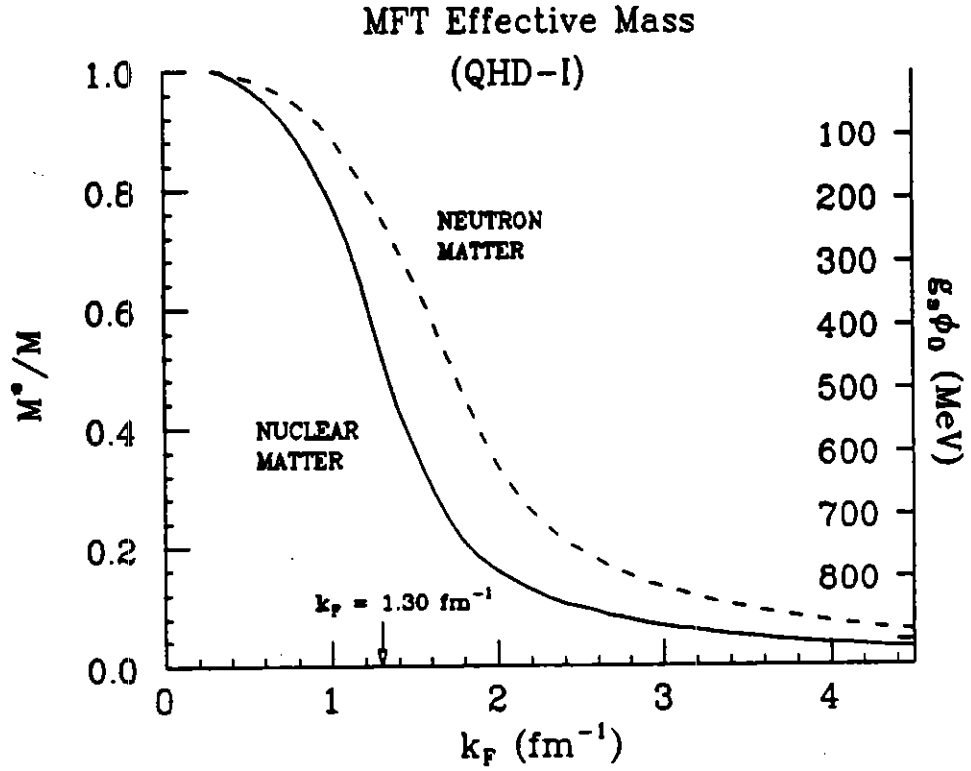

Figure 2: Effective mass M^*/M as a function of density for nuclear ($\gamma = 4$) and neutron ($\gamma = 2$) matter based on fig. 1.

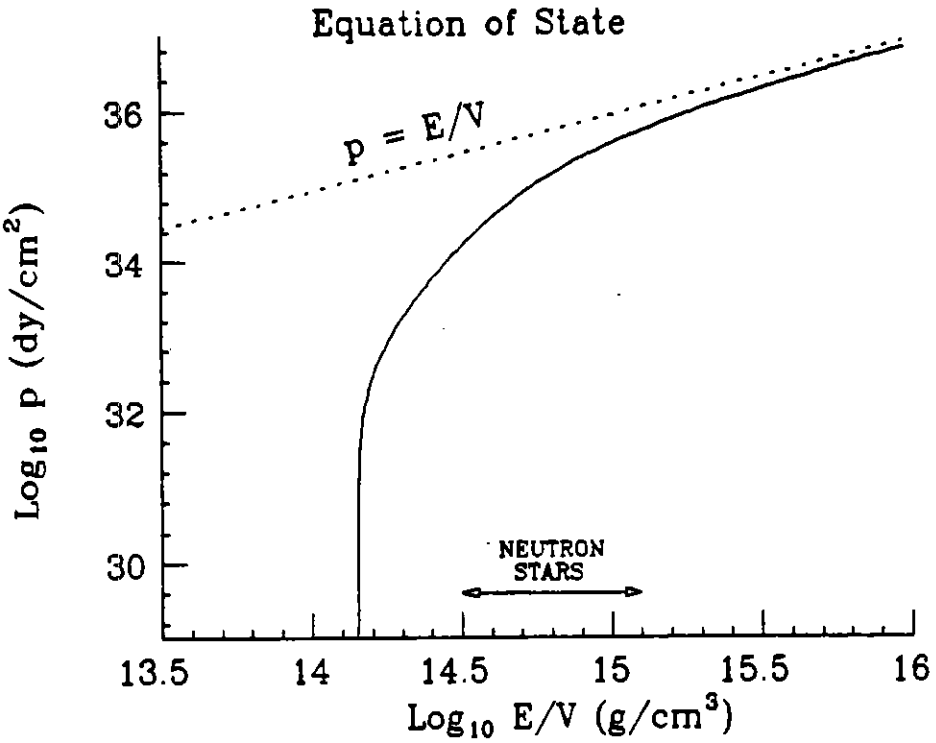

Figure 3: Predicted equation of state for neutron matter at all densities. The dotted line represents the causal limit $p = \mathcal{E}$. The density regime relevant for neutron stars is also shown.

"causal limit" $p = \mathcal{E}$ representing the stiffest possible equation of state. Thus we have a simple, two-parameter model that is consistent with the equilibrium point of normal nuclear matter and that allows for a covariant, causal extrapolation to any density.

The neutron matter equation of state shown in fig. 3 can be used in the Tolman-Oppenheimer-Volkoff equation for the general-relativistic metric[33] to give the masses of neutron stars as a function of the central density. This MFT gives a maximum neutron star mass of $\approx$ 2.6 solar masses; this is large enough to accommodate the largest observed neutron stars, which contain roughly 1.5 solar masses. The density at the center of the star is approximately six times larger than the central density in ^{208}Pb, and the asymptotic approach of the equation of state to the causal limit is already relevant in this regime. Moreover, although the low-density behavior of nuclear matter is sensitive to the nearly exact cancellation between attractive scalar and repulsive vector components, the stiff high-density equation of state is determined simply by the Lorentz structure of the interaction; the scalar attraction saturates completely at high densities, producing an essentially massless gas of baryons interacting through a strong vector repulsion, which leads to a stiff equation of state.[34] Note that the onset of the asymptotic regime occurs at densities similar to those in the interiors of neutron stars.

Finite Nuclei

We now generalize the results of the preceding subsection to study atomic nuclei. We continue to work in the mean-field approximation to QHD-I, but since the system

now has finite spatial extent, these fields are spatially dependent. If we initially restrict consideration to spherically symmetric nuclei, the meson fields depend only on the radius, and since the baryon current is conserved, the spatial part of the vector field $\mathbf{V}$ again vanishes.[7] Thus the mean-field QHD–I lagrangian of eq. (8) becomes

$$\mathcal{L}^{(\mathrm{I})}_{\mathrm{MFT}} = \overline{\psi}[i\gamma_\mu\partial^\mu - g_{\mathrm{v}}\gamma_0 V_0 - (M - g_{\mathrm{s}}\phi_0)]\psi - \tfrac{1}{2}[(\nabla\phi_0)^2 + m_{\mathrm{s}}^2\phi_0^2] + \tfrac{1}{2}[(\nabla V_0)^2 + m_{\mathrm{v}}^2 V_0^2]\,, \quad (22)$$

and the Dirac equation for the baryon field is

$$\Big\{i\gamma_\mu\partial^\mu - g_{\mathrm{v}}\gamma_0 V_0(r) - [M - g_{\mathrm{s}}\phi_0(r)]\Big\}\psi(x) = 0\,. \quad (23)$$

Appropriate values for the scalar and vector couplings (g_{s} and g_{v}) and masses (m_{s} and m_{v}) will be given below.

Although the baryon field is still an operator, the meson fields are classical; hence eq. (23) is linear, and we may again seek normal-mode solutions of the form $\psi(x) = \psi(\mathbf{x})\,\mathrm{e}^{-iEt}$. This leads to the eigenvalue equation

$$h\psi(\mathbf{x}) \equiv \{-i\boldsymbol{\alpha}\cdot\boldsymbol{\nabla} + g_{\mathrm{v}}V_0(r) + \beta[M - g_{\mathrm{s}}\phi_0(r)]\}\psi(\mathbf{x}) = E\psi(\mathbf{x})\,, \quad (24)$$

which defines the single-particle Dirac hamiltonian h. Equation (24) has both positive- and negative-energy solutions $\mathcal{U}(\mathbf{x})$ and $\mathcal{V}(\mathbf{x})$, which allow the field operators to be constructed in the Schrödinger picture. The positive-energy spinors can be written as

$$\mathcal{U}_\alpha(\mathbf{x}) \equiv \mathcal{U}_{n\kappa mt}(\mathbf{x}) = \begin{pmatrix} i\big[G_{n\kappa t}(r)/r\big]\Phi_{\kappa m} \\ -\big[F_{n\kappa t}(r)/r\big]\Phi_{-\kappa m}\end{pmatrix}\zeta_t\,, \quad (25)$$

where n is the principal quantum number, $\Phi_{\kappa m}$ is a spin-1/2 spherical harmonic:[35]

$$\Phi_{\kappa m} = \sum_{m_\ell m_{\mathrm{s}}} \langle \ell m_\ell \tfrac{1}{2} m_{\mathrm{s}} | \ell \tfrac{1}{2} j m\rangle Y_{\ell,m_\ell}(\Omega)\chi_{m_{\mathrm{s}}}\,, \quad (26)$$

$$j = |\kappa| - \tfrac{1}{2}\,, \qquad \ell = \begin{cases} \kappa\,, & \kappa > 0\,, \\ -(\kappa+1)\,, & \kappa < 0\,, \end{cases} \quad (27)$$

and ζ_t is a two-component isospinor labeled by the isospin projection t. (We take $t = \frac{1}{2}$ for protons and $t = -\frac{1}{2}$ for neutrons.) The phase choice in eq. (25) produces real bound-state wave functions F and G for real potentials ϕ_0 and V_0, and the normalization is given by

$$\int_0^\infty \mathrm{d}r\Big(|G_\alpha(r)|^2 + |F_\alpha(r)|^2\Big) = 1\,, \quad (28)$$

which ensures unit probability to find each nucleon somewhere in space.

The classical meson field equations follow from eq. (22) and resemble eqs. (3) and (4) restricted to static, spherically symmetric fields. With the general form for the spinors in eq. (25), we can evaluate the nuclear densities, which serve as source terms in the meson field equations. Assume that the nuclear ground state consists of filled shells up to some value of n and κ, which may be different for protons and neutrons; this is appropriate for doubly magic nuclei. In addition, assume that all bilinear products of

baryon operators are normal ordered, which removes contributions from the negative-energy spinors $\mathcal{V}_\alpha(\mathbf{x})$. This amounts to neglecting the filled Dirac sea of baryons and defines the mean-field approximation. The zero-point terms arising from $\mathcal{V}_\alpha(\mathbf{x})$ will be included later.

With these assumptions, the local baryon (ρ_B) and scalar (ρ_s) densities become

$$\left.\begin{matrix}\rho_B(\mathbf{x})\\ \rho_s(\mathbf{x})\end{matrix}\right\} = \sum_\alpha^{\text{occ}} \overline{\mathcal{U}}_\alpha(\mathbf{x}) \begin{pmatrix}\gamma^0\\ 1\end{pmatrix} \mathcal{U}_\alpha(\mathbf{x}) = \sum_a^{\text{occ}} \left(\frac{2j_a+1}{4\pi r^2}\right)\left(|G_a(r)|^2 \pm |F_a(r)|^2\right), \tag{29}$$

which holds for filled shells, as appropriate for spherically symmetric nuclei. The remaining quantum numbers are denoted by $\{\alpha\} = \{a; m\} \equiv \{n, \kappa, t; m\}$. Notice that since the shells are filled, the sources are spherically symmetric.

The sources produce the meson fields, which satisfy static Klein–Gordon equations:

$$\frac{\mathrm{d}^2}{\mathrm{d}r^2}\phi_0(r) + \frac{2}{r}\frac{\mathrm{d}}{\mathrm{d}r}\phi_0(r) - m_s^2\phi_0(r) = -g_s\rho_s(r), \tag{30}$$

$$\frac{\mathrm{d}^2}{\mathrm{d}r^2}V_0(r) + \frac{2}{r}\frac{\mathrm{d}}{\mathrm{d}r}V_0(r) - m_v^2 V_0(r) = -g_v\rho_B(r). \tag{31}$$

The equations for the baryon wave functions follow upon substituting eq. (25) into eq. (24), which produces

$$\frac{\mathrm{d}}{\mathrm{d}r}G_a(r) + \frac{\kappa}{r}G_a(r) - \left[E_a - g_v V_0(r) + M - g_s\phi_0(r)\right]F_a(r) = 0, \tag{32}$$

$$\frac{\mathrm{d}}{\mathrm{d}r}F_a(r) - \frac{\kappa}{r}F_a(r) + \left[E_a - g_v V_0(r) - M + g_s\phi_0(r)\right]G_a(r) = 0. \tag{33}$$

Thus the spherical nuclear ground state is described by coupled, ordinary differential equations that may be solved by an iterative procedure, as discussed in ref. 36. They contain all information about the static ground-state nucleus in this approximation.

The mean-field hamiltonian can be computed just as for infinite matter, and after normal ordering, the ground-state energy is given by

$$E = \int \mathrm{d}^3x \left\{\frac{1}{2}\left[(\nabla\phi_0)^2 + m_s^2\phi_0^2\right] - \frac{1}{2}\left[(\nabla V_0)^2 + m_v^2 V_0^2\right] + \sum_\alpha^{\text{occ}} \mathcal{U}_\alpha^\dagger(\mathbf{x})\left[-i\boldsymbol{\alpha}\cdot\nabla + \beta(M - g_s\phi_0) + g_v V_0\right]\mathcal{U}_\alpha(\mathbf{x})\right\}. \tag{34}$$

Here the meson fields are functions of the radial coordinate, and $\boldsymbol{\alpha}$ and β are the usual Dirac matrices. Notice that if we interpret this expression as an *energy functional* for the Dirac–Hartree ground state, extremization with respect to the meson fields reproduces the field equations (30) and (31), with the densities from eq. (29). Moreover, extremization with respect to the baryon wave functions $\mathcal{U}_\alpha^\dagger(\mathbf{x})$, subject to the constraint

$$\int \mathrm{d}^3x\, \mathcal{U}_\alpha^\dagger(\mathbf{x})\mathcal{U}_\alpha = 1 \tag{35}$$

for all occupied states (which is enforced by Lagrange multipliers E_α), leads to the Dirac equation (24). This alternative derivation of the Dirac–Hartree equations from an energy functional is useful for extensions of the simple model discussed in this subsection.

Once the solutions to the Dirac–Hartree equations have been found, the ground-state energy (34) can be computed by using the Dirac equation (24) to introduce the eigenvalues E_α and by partially integrating the meson terms to introduce the densities. In the end, the total energy of the system is given by

$$E = \sum_{\alpha}^{\text{occ}} E_\alpha (2j_\alpha + 1) - \frac{1}{2}\int \mathrm{d}^3x \left[-g_s \phi_0(r)\rho_s(r) + g_v V_0(r)\rho_B(r) \right] . \tag{36}$$

Before discussing the Dirac–Hartree solutions, let us generalize the equations to include some additional degrees of freedom and couplings. Although the isoscalar meson fields are the most important for describing general properties of nuclear matter, a quantitative comparison with actual nuclei requires the introduction of some additional dynamics.

For example, it is necessary to include the electromagnetic interaction to account for the Coulomb repulsion between protons. Moreover, since hadronic interactions exhibit an almost exact SU(2) isospin symmetry, the nucleons can couple to isovector mesons in addition to the isoscalar (neutral) mesons of QHD–I. These isovector mesons, for example the π and ρ, come in three charge states (+, 0, −) and couple differently to the proton and neutron. Thus they affect the nuclear symmetry energy, which arises when there are unequal numbers of neutrons and protons.

The construction of a renormalizable lagrangian containing charged, massive vector fields is somewhat complicated and is discussed at length in Abers and Lee;[37] applications to the present model can be found in ref. 7. For our purposes, we require only the classical contributions from these fields, and in this case, the lagrangian simplifies considerably. In particular, since the nuclear ground state has well-defined charge, only the neutral ρ meson field (denoted by b_0) enters, and since the ground state is assumed to have well-defined parity and spherical symmetry, there is no classical π field. Thus the mean-field lagrangian for this extended model, which is called QHD–II, is given by

$$\begin{aligned} \mathcal{L}^{(\mathrm{II})}_{\mathrm{MFT}} = \overline{\psi}[i\gamma_\mu\partial^\mu - g_v\gamma_0 V_0 - \tfrac{1}{2}g_\rho\tau_3\gamma_0 b_0 - e\tfrac{1}{2}(1+\tau_3)\gamma_0 A_0 - (M - g_s\phi_0)]\psi \\ - \tfrac{1}{2}[(\nabla\phi_0)^2 + m_s^2\phi_0^2] + \tfrac{1}{2}[(\nabla V_0)^2 + m_v^2 V_0^2] \\ + \tfrac{1}{2}(\nabla A_0)^2 + \tfrac{1}{2}[(\nabla b_0)^2 + m_\rho^2 b_0^2] . \end{aligned} \tag{37}$$

Here A_0 is the Coulomb potential, e is the proton electromagnetic charge, g_ρ is the rho-nucleon coupling constant, and τ_i are the usual isospin Pauli matrices. For now, all of the boson fields are assumed to be functions of the radial coordinate only.

The Dirac–Hartree equations for this extended model can be derived just as before. The Dirac equations for the baryon wave functions now contain b_0 and A_0, and because of the structure of the τ_3 matrix, b_0 couples with opposite sign to protons and neutrons, and A_0 couples only to the protons. In addition to the source terms in eq. (29), which

Table 1:
Dirac–Hartree Parameter Sets
(All sets use $M = 939$ MeV and $m_v \equiv m_\omega = 783$ MeV.)

Set	g_s^2	g_v^2	g_ρ^2	m_s (MeV)	κ/M	λ
L1	91.64	136.2	36.79	550.	0	0
L2	109.6	190.4	65.23	520.	0	0
NLB	94.01	158.48	73.00	510.	0.852	10
RHA0	53.78	102.58	83.30	456.	0	0

sum over both proton and neutron occupied states, the source term for the ρ meson involves the *difference* between proton and neutron densities, while the Coulomb source involves only protons. These different types of couplings allow for a more accurate reproduction of real nuclei, where the proton and neutron wave functions are not identical. The full set of equations are presented in ref. 7 and are used to compute the results discussed below.

Spherical Nuclei. The solutions of the preceding equations depend on the parameters g_s, g_v, m_s, and g_ρ (when the ρ meson is included). We take the experimental values $M = 939$ MeV, $m_v \equiv m_\omega = 783$ MeV, $m_\rho = 770$ MeV, and $e^2/4\pi = \alpha = 1/137.0$ (which determines the Coulomb potential) as fixed. The free parameters are chosen so that when the Dirac–Hartree equations are solved in the limit of infinite nuclear matter, the empirical equilibrium density ($\rho_B^0 = 0.1484$ fm^{-3}), binding energy (15.75 MeV), and symmetry energy (35 MeV) are reproduced. The empirical equilibrium density ρ_B^0 is determined here from the density in the interior of ^{208}Pb and corresponds to $k_F^0 = 1.3\,\mathrm{fm}^{-1}$. We also fit the empirical rms charge radius of ^{40}Ca ($r_{rms} = 3.482$ fm), which is determined primarily by m_s. This procedure produces the parameters in the row labeled L2 in table 1, which are taken from ref. 36. This parameter set yields the same values for C_s^2 and C_v^2 as in eq. (21), so that $M^*/M = 0.541$ and $K \approx 545$ MeV at nuclear matter equilibrium.

Once the parameters have been specified, the properties of all closed-shell nuclei are determined in this approximation. For example, figs. 4, 5, and 6 show the Dirac–Hartree charge densities of ^{16}O, ^{40}Ca, and ^{208}Pb compared with two nonrelativistic calculations[2,38] and the empirical distributions determined from electron scattering.[39–41] The empirical proton charge form factor has been folded with the calculated "point proton" density to determine the charge density. Similar results are obtained for other closed-shell nuclei.[36,42] Evidently, the nonrelativistic and relativistic calculations agree with the data at about the same level of accuracy.

In fig. 7, the predicted energy levels in ^{208}Pb are compared with experimental values derived from neighboring nuclei.[43,44] The relativistic calculations clearly reveal a shell structure. This arises from the spin-orbit interaction that occurs naturally when

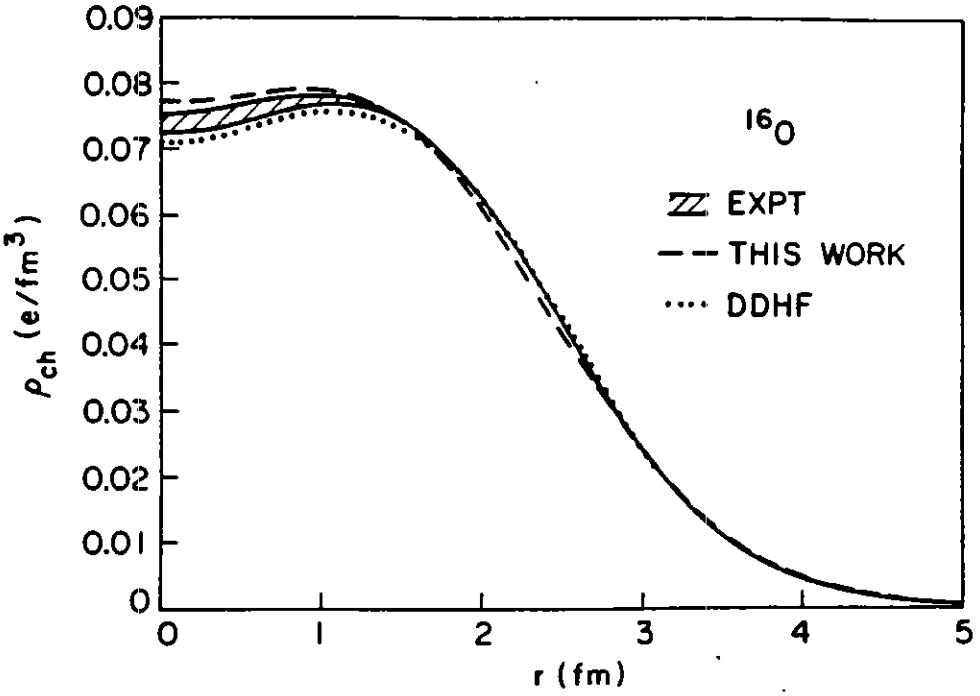

Figure 4: Charge density distribution for ^{16}O. Dirac–Hartree results are indicated by the dashed line. The experimental curve is from ref. 39, and the dotted curve shows the Density-Dependent Hartree–Fock (DDHF) results of Negele.[38]

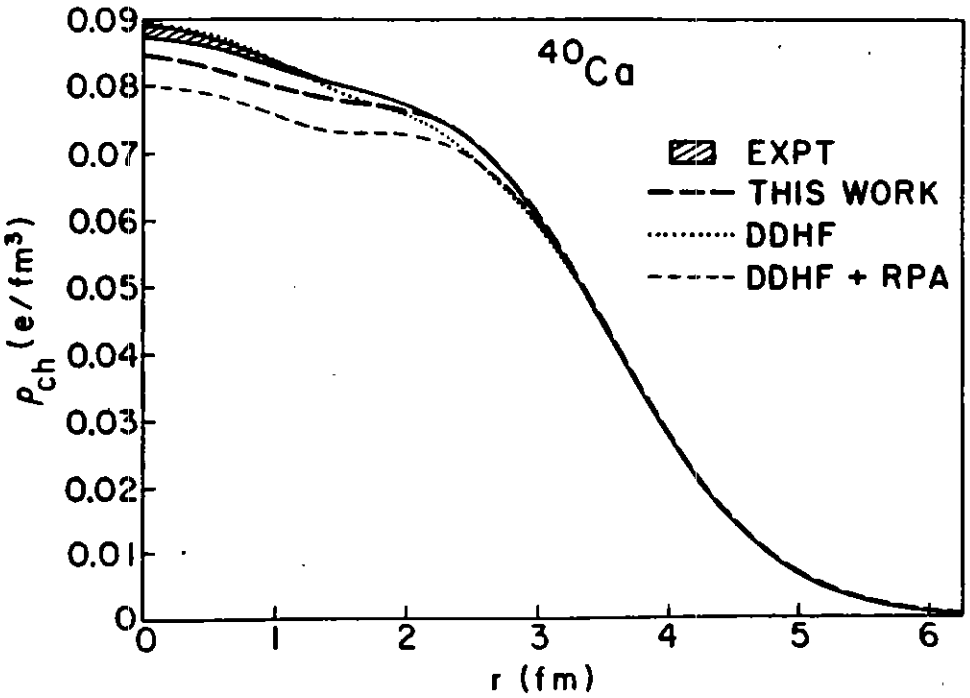

Figure 5: Charge density distribution for ^{40}Ca. The experimental curve is from Sick *et al.*[41] The DDHF results are those of Negele, and the DDHF + RPA calculation is that of Gogny, as indicated in ref. 41. The Dirac–Hartree calculations yield the long-dashed curve.

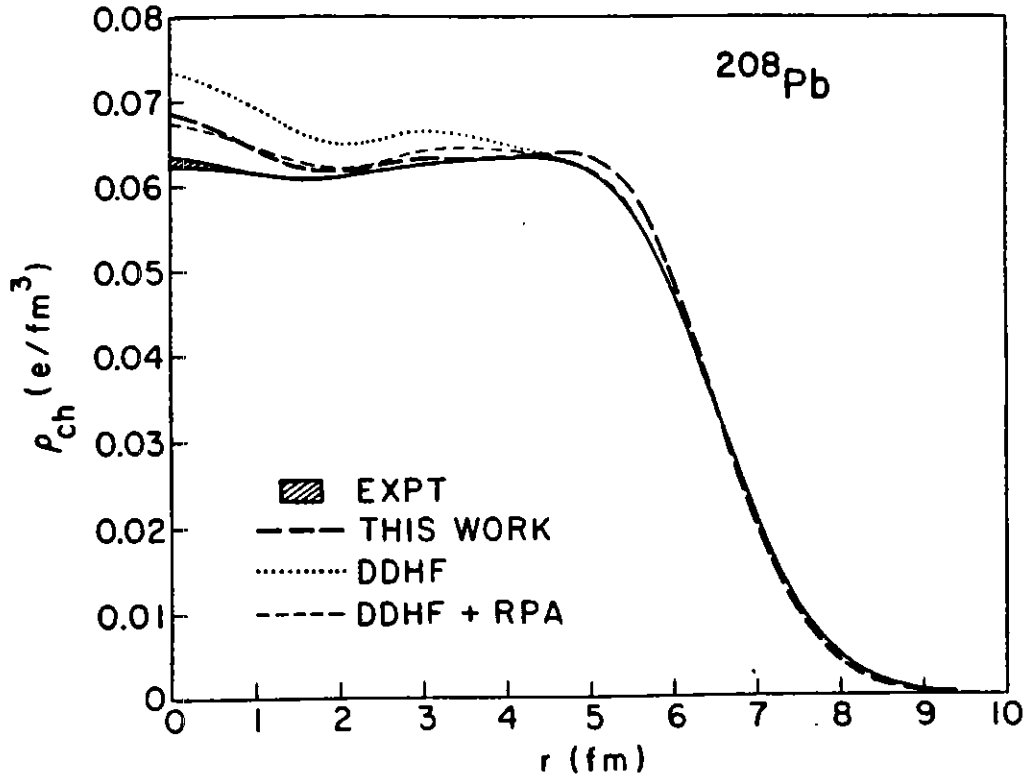

Figure 6: Charge density distribution for ^{208}Pb. The solid curve and shaded region represent the fit to experimental data in ref. 40. Dirac-Hartree results are indicated by the long-dashed line. The DDHF calculations of Gogny[2] are also shown.

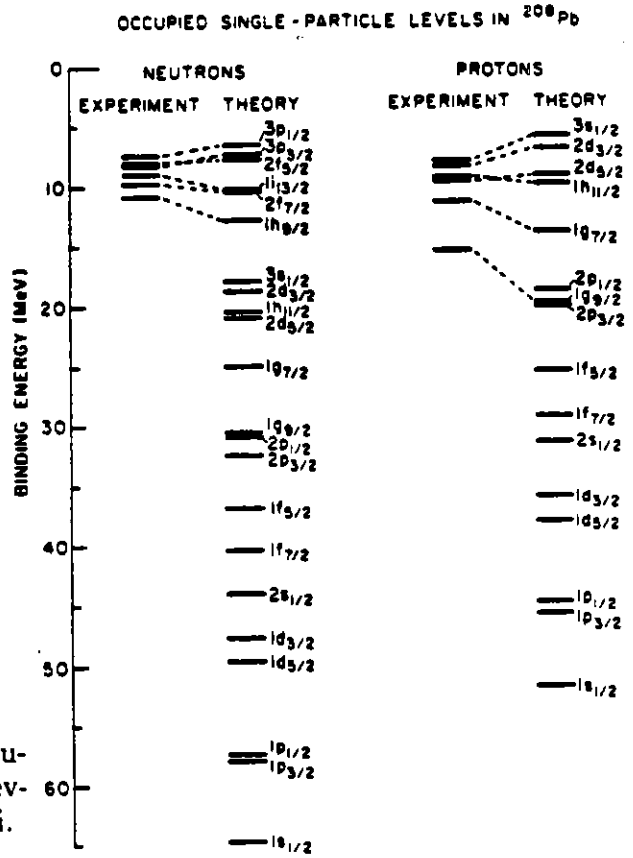

Figure 7: Predicted spectrum for occupied levels in ^{208}Pb. Experimental levels are taken from neighboring nuclei.

a Dirac particle moves in large classical scalar and vector fields.[45–47] Note that whereas $g_s\phi_0$ and $g_v V_0$ tend to cancel in the central potential that determines saturation, they add constructively in the spin-orbit potential. We emphasize that no parameters are adjusted specifically to produce the spin-orbit interaction, as is usually the case in non-relativistic calculations. Thus, with a minimal number of phenomenological parameters determined from bulk nuclear properties, *one derives the existence of the nuclear shell model.*

There are several attractive features in this relativistic model of nuclear structure. First, the calculation of the nuclear ground state is self-consistent. The scalar and vector fields follow directly from the scalar and baryon densities, which are in turn determined by the solutions to the Dirac equation (24) in the classical fields. Second, only four adjustable parameters specify the properties of all closed-shell nuclei in this approximation. Finally, this relativistic shell model is simply one piece of a consistent many-body framework based on QHD. One can therefore systematically investigate corrections to the nuclear ground state, such as those arising from the filled Dirac sea of negative-energy states, as we describe below.

Deformed Nuclei. To study the systematics of this relativistic model of nuclear structure, we extend the preceding equations to deal with deformed, axially symmetric nuclei. This allows us to calculate not only the ground states of nuclei with fully closed shells, but also those for even-even nuclei between closed shells. We will concentrate here on nuclei with $12 \leq B \leq 40$, which includes the $1p$ and $2s$–$1d$ shells.[48] The restriction to azimuthal and reflection-symmetric deformations is reasonable for light, even-even nuclei.

These assumed symmetries of the ground state, together with the assumption of well-defined parity, imply that the nonvanishing meson fields are the same ones that appear in spherical nuclei.[49] Thus the Dirac–Hartree equations are essentially the same as those written earlier, except that all fields now depend on both a radial and an angular coordinate [for example, $\phi_0(r,\theta)$], and all the differential equations become partial differential equations. The source densities are still computed as in eq. (29), but they now depend on r and θ. There are several methods for solving the resulting set of coupled partial differential equations, and the interested reader is directed to the literature for a discussion.[50–52] The equilibrium deformation is obtained by choosing the occupied single-particle states to minimize the energy.

In fig. 8, we show the results of Furnstahl, Price, and Walker for quadrupole moments in the $2s$–$1d$ shell.[52] The parameter sets used are listed as L2 and NLB in table 1; the latter includes scalar-meson self-couplings of the form

$$V(\phi) = \frac{\kappa}{3!}\phi^3 + \frac{\lambda}{4!}\phi^4 \tag{38}$$

in the model lagrangian. (These new couplings allow for some "fine tuning" of the bulk nuclear properties.) Both of these sets produce nuclear saturation at $k_F^0 = 1.30\,\mathrm{fm}^{-1}$ with a binding energy of 15.75 MeV and a symmetry energy of 35 MeV, and they

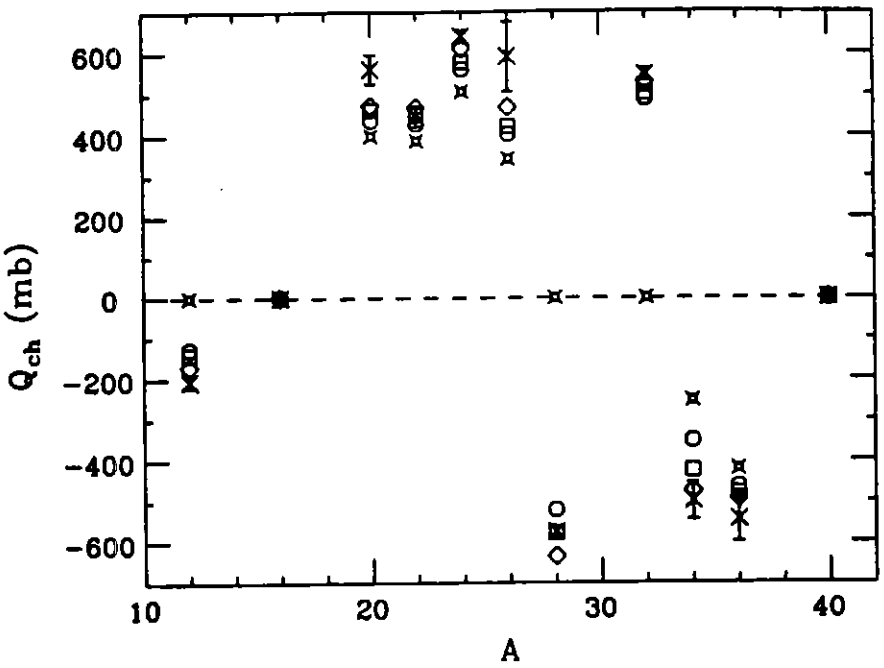

Figure 8: Intrinsic charge quadrupole moment (mb) in even-even s–d nuclei for parameter sets L2 (stars) and NLB (circles) taken from table 1. The results shown by squares and diamonds follow from similar parameter sets given in ref. 52. Moments derived from experimental measurements of $B(E2)$ values ($\times$) are taken from Leander and Larsson.[53]

also generate the correct rms radius for ^{40}Ca, just as for the spherical calculations in the preceding subsection. Nevertheless, these two sets produce slightly different values of M^* in nuclear matter ($M^*/M = 0.54$ for L2 and $M^*/M = 0.61$ for NLB), which is sufficient to produce different results for the deformation of nuclei with closed subshells. (The deformation depends sensitively on the level density near the Fermi surface, which is determined essentially by the inverse of M^*.) Observe that set L2 predicts spherical shapes for ^{12}C, ^{28}Si, and ^{32}S, in contradiction to experiment. In contrast, the small modifications afforded by the couplings κ and λ in set NLB lead to excellent agreement with the experimental moments, particularly the systematic trends and the oscillation between oblate and prolate shapes around $B = 32$, while leaving the results for spherical nuclei essentially unchanged. Thus the successful description of spherical nuclei in this relativistic model can be extended to reproduce the observed systematics of light deformed nuclei *with the same parameters*. Finally, the relativistic results are very similar to those obtained from nonrelativistic Skyrme–Hartree–Fock calculations[54] that also use an interaction fitted to nuclear properties.

Nucleon–Nucleus Scattering

The scattering of medium-energy nucleons from nuclei can provide information about both nuclear structure and the nucleon–nucleon (NN) interaction. Since the NN inter-

action has complex spin, isospin, momentum, and density dependence, nucleon–nucleus scattering exhibits a wide variety of phenomena. As a starting point for describing these phenomena, we use the Dirac–Hartree description of the nucleus, together with the Relativistic Impulse Approximation (RIA), which assumes that the interaction between the projectile and target nucleons has essentially the same form as the interaction between two nucleons in free space. This interaction is used to produce a nucleon–nucleus optical potential that incorporates the leading term in a multiple-scattering series.

Although the simple QHD models discussed above are useful for studying the average properties of the nuclear interaction, they are less useful for describing the detailed quantitative features (such as spin dependence) of the full NN scattering amplitude. These quantitative features are important for any reasonable description of the nucleon–nucleus scattering observables. The RIA allows us to combine the empirical free-space scattering amplitude with a relativistic calculation of the nuclear ground state.

The RIA as originally formulated[4–6] involves two basic procedures. First, the experimental NN scattering amplitude is represented by a particular set of five Lorentz covariant functions[55] that multiply the so-called "Fermi invariant" Dirac matrices. The Lorentz covariant functions are then folded with the Dirac–Hartree target densities to produce a first-order optical potential for use in the Dirac equation for the projectile. We briefly summarize the formalism and then compare observables computed in the RIA with experimental data and with nonrelativistic impulse approximation calculations.

The constraints of Lorentz covariance, parity conservation, isospin invariance, and that free nucleons are on their mass shell imply that the invariant NN scattering operator $\mathcal{F}$ can be written in terms of five complex functions for *pp* scattering and five for *pn* scattering. In the original RIA, $\mathcal{F}$ was taken as[7]

$$\mathcal{F} = \mathcal{F}^S + \mathcal{F}^V \gamma^\mu_{(0)} \gamma_{(1)\mu} + \mathcal{F}^{PS} \gamma^5_{(0)} \gamma^5_{(1)} + \mathcal{F}^T \sigma^{\mu\nu}_{(0)} \sigma_{(1)\mu\nu} + \mathcal{F}^A \gamma^5_{(0)} \gamma^\mu_{(0)} \gamma^5_{(1)} \gamma_{(1)\mu} , \qquad (39)$$

where the subscripts (0) and (1) refer to the incident and struck nucleons, respectively. Each amplitude $\mathcal{F}^L$ is a complex function of the Lorentz invariants t (four-momentum transfer squared) and s (total four-momentum squared), or equivalently, of the momentum transfer q and incident energy E. It is found empirically that the amplitudes $\mathcal{F}^S$, $\mathcal{F}^V$, and $\mathcal{F}^{PS}$ are much larger than any amplitudes obtained in a nonrelativistic decomposition, which uses Galilean-invariant operators.

The RIA optical potential $U_{\rm opt}(q, E)$ is defined as

$$U_{\rm opt}(q, E) = -\frac{4\pi i p}{M} \langle \Psi | \sum_{n=1}^{A} e^{i\mathbf{q}\cdot\mathbf{x}(n)} \mathcal{F}(q, E; n) | \Psi \rangle , \qquad (40)$$

where $\mathcal{F}$ is the scattering operator of eq. (39), p is the magnitude of the projectile three-momentum in the nucleon–*nucleus* cm frame (where the scattering observables will be calculated), $|\Psi\rangle$ is the A-particle nuclear ground state, and the sum runs over all nucleons in the target. $\mathcal{F}$ is a function of the momentum transfer q and collision energy E, which we take to be the cm energy for a stationary target nucleon and incident proton at the laboratory energy; this amounts to neglecting nuclear recoil.

With these simplifications, the Dirac optical potential is local, and only diagonal nuclear densities are needed. For a spin-zero nucleus, the only nonzero densities are the baryon and scalar densities of eq. (29), plus a tensor term computed by inserting σ^{0i} between the spinors in eq. (29). Thus the optical potential takes the form

$$U_{\rm opt} = U^S + \gamma^0 U^V - 2i\boldsymbol{\alpha}\cdot\hat{\boldsymbol{r}}U^T\,, \tag{41}$$

where $U^L \equiv U^L(r;E)$ for each component. The tensor contribution U^T is small and will be neglected in what follows. The RIA optical potential then has only scalar and vector contributions, and the Dirac equation for the projectile has precisely the same form as eq. (24), with U^V replacing $g_v V_0$ and U^S replacing $(-g_s\phi_0)$:

$$h\mathcal{U}_0(\mathbf{x}) = \Big\{-i\boldsymbol{\alpha}\cdot\boldsymbol{\nabla} + U^V(r;E) + \beta\big[M + U^S(r;E)\big]\Big\}\mathcal{U}_0(\mathbf{x}) = E\mathcal{U}_0(\mathbf{x})\,. \tag{42}$$

In practice, one includes in U^V the Coulomb potential computed from the empirical nuclear charge density; other electromagnetic contributions arising from the proton anomalous magnetic moment are of similar size to the tensor term U^T and are neglected here.

For proton scattering from a spin-zero target, three relevant observables may be defined in terms of the proton–nucleus scattering amplitude $T(\theta) = g(\theta) + h(\theta)\,\boldsymbol{\sigma}\cdot\hat{\boldsymbol{n}}$. These are the differential cross section σ, the polarization (or analyzing power) P, and the spin-rotation function Q:

$$\sigma = |g|^2 + |h|^2\,, \tag{43}$$

$$P = 2\,\mathrm{Re}(gh^*)/(|g|^2 + |h|^2)\,, \tag{44}$$

$$Q = 2\,\mathrm{Im}(gh^*)/(|g|^2 + |h|^2)\,. \tag{45}$$

In fig. 9, RIA results for proton scattering from ^{40}Ca are shown as solid curves. The target densities are taken from the results for spherical nuclei discussed above, ***with no further adjustment of parameters.*** The RIA results are compared with nonrelativistic impulse approximation calculations (dashed curves) carried out in the conventional Kerman–McManus–Thaler formalism.[56] Evidently, the RIA calculations agree remarkably well with the data. Moreover, although more sophisticated nonrelativistic calculations give better agreement with the data, the relativistic results are superior, particularly for the spin observables, when the impulse approximation is used for both.

The spin dynamics is inherent in the relativistic formalism and arises naturally from the large Lorentz scalar and vector potentials in the Dirac equation (42). This is precisely the same spin dynamics that produces the observed spin-orbit splittings in the bound single-particle levels. *Thus the relativistic Hartree calculations provide a minimal unifying theoretical basis for both the nuclear shell model and medium-energy proton–nucleus scattering—two essential aspects of nuclear physics.*

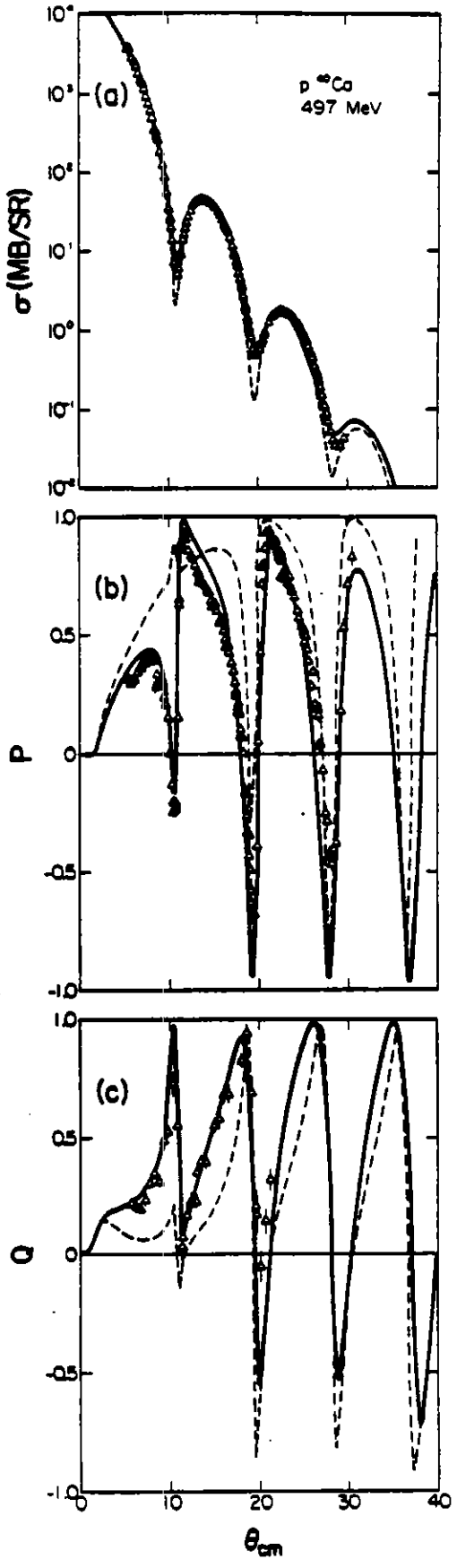

Figure 9: Calculated cross section (a), analyzing power (b), and spin-rotation function (c) for $p+^{40}$Ca at a laboratory kinetic energy of 497 MeV. The RIA results are given by the solid curves, while the dashed curves follow from a nonrelativistic impulse approximation calculation.[7]

Nuclear Excited States

We now turn to the calculation of nuclear response functions and the properties of nuclear excited states, as described in the random-phase approximation (RPA) built on the MFT ground state. These excitations arise from the consistent linear response of the ground state, in which the nucleons move coherently in varying classical meson fields that are in turn determined by oscillatory nuclear sources. Many studies of the relativistic nuclear response have been carried out for both infinite matter and finite nuclei, beginning with the pioneering work of Chin,[57] and here we will focus on two issues. The first is the importance of consistency, which implies that the particle-hole interaction in the excited states must be the same (and use the same parameter values) as the interaction in the ground state. This is important for producing a reasonable excitation spectrum when the underlying interaction involves a sensitive cancellation between large attractive and repulsive components. Second, we will see that the relativistic response involves not only the familiar positive-energy particle-hole configurations, but also configurations that mix positive- and negative-energy states. These new configurations are crucial for the conservation of the electromagnetic current and the separation of the "spurious" $J^\pi = 1^-$ state. This emphasizes that the Dirac single-particle basis is complete only when both positive- and negative-energy states are included.

The calculation of the linear response is basically the same as in nonrelativistic many-body theory.[48] The principal idea is to compute the particle-hole (polarization) propagator and to extract the collective excitation energies and transition amplitudes from the poles and residues of this propagator. Several methods have been developed and applied to finite nuclei.[58–61] Existing results are restricted primarily to isoscalar excitations, because fitting the bulk nuclear properties constrains only the isoscalar particle-hole interaction significantly and because the isovector response depends critically on pion dynamics, with the associated complexity that we discuss later. An excellent discussion of the role of consistency is contained in the work of Dawson and Furnstahl,[61] whose results we quote here.

In fig. 10 the low-lying, negative-parity, isoscalar states in ^{16}O are compared to several empirical levels that might be reasonably described as particle-hole excitations. (Only the lowest state of each J is shown.) The first column shows the unperturbed excitation energy with the spectrum determined from the ground-state calculation using the parameter set L2 in table 1. The second column contains the RPA spectrum when only positive-energy particle-hole configurations are allowed, and the third column gives the spectrum when negative-energy states are also included. Notice that the full RPA results agree favorably with the empirical values in the fourth column, which is a nontrivial result because of the large cancellations between scalar and vector contributions. Moreover, it is clear that the negative-energy states play an important role in determining the RPA spectrum, particularly for the spurious 1^- state. Lorentz covariance implies that in a consistent RPA calculation, this state should appear at zero excitation energy, which occurs only when the full Dirac basis is maintained.

Figure 11, taken from a calculation by Furnstahl,[62] shows the relativistic RPA result

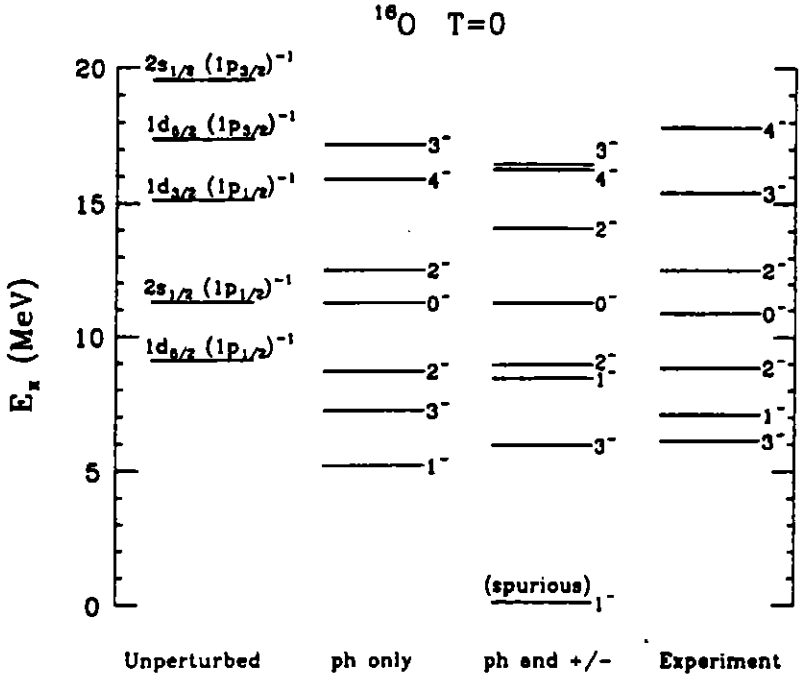

Figure 10: Energy levels of selected low-lying states in ^{16}O in a spectral RPA calculation. The spurious 1^-0 state does not appear in the second column, since its eigenvalue is imaginary when only particle-hole configurations are included.

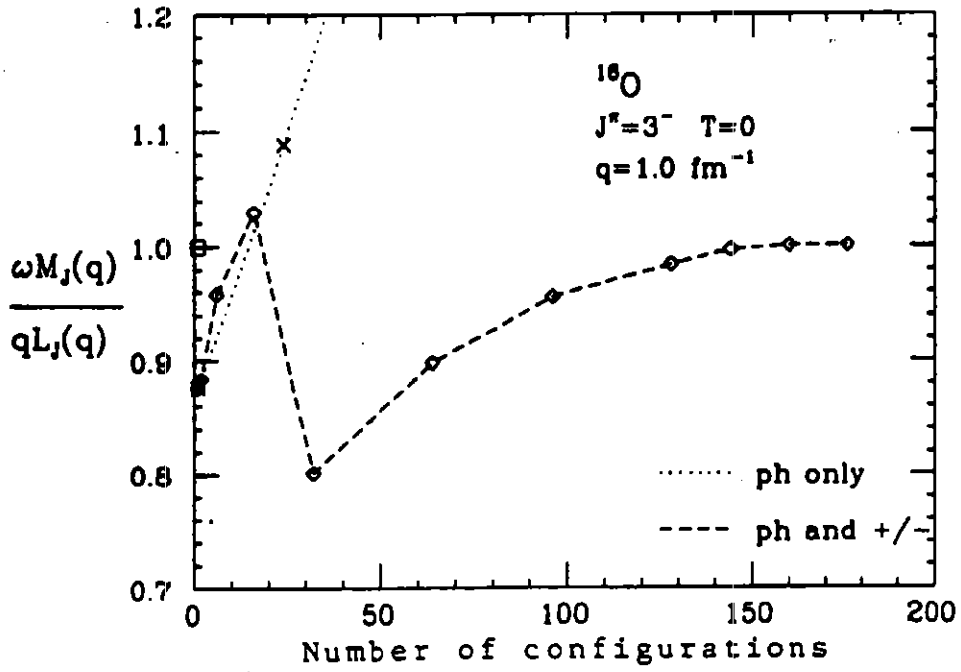

Figure 11: The ratio of transition charge and longitudinal current densities for the low-lying isoscalar 3^- state in ^{16}O in a spectral RPA calculation, as a function of the configuration space size. The densities are evaluated at q = 1.0 fm^{-1}.

for the ratio of the transition charge density to the longitudinal current density for a particular transition in ^{16}O. The results are plotted as function of the number of configurations, and if the electromagnetic current is conserved, the ratio should be unity. The dotted curve includes only the positive-energy configurations, and the current is evidently not conserved. In contrast, the dashed curve gives the result of the full RPA calculation, including the negative-energy states. The conclusion from this figure is that it is *essential* to include all states in the Dirac basis to maintain the conservation of the current.

The Role of the Quantum Vacuum

We have thus far studied the consequences of the mean-field hamiltonian of eq. (12) and its generalization to finite nuclei. Let us now return to infinite nuclear matter and include the contribution from δH in eq. (13), which defines the relativistic Hartree approximation or RHA. (This is also often called the one-loop approximation.) These contributions are an integral part of a fully relativistic description of nuclear structure, and as we have just seen, it is impossible to construct a meaningful nuclear response or consistent nuclear currents without including the negative-energy states. Thus, although the MFT ground state is covariant, causal, and internally consistent by itself, it is hard to justify the omission of the negative-energy contributions.

An inspection of δH reveals that, even with the indicated vacuum subtraction, the sum still diverges. Since the model QHD-I is renormalizable, however, the sum can be rendered finite by including counterterms in the lagrangian (8). These counterterms also appear in the hamiltonian, and they can be grouped with δH, resulting in a correction to the energy density of the form

$$\Delta\mathcal{E}(M^*) = -\frac{1}{V}\sum_{\mathbf{k}\lambda}\Big[(\mathbf{k}^2+M^{*2})^{1/2}-(\mathbf{k}^2+M^2)^{1/2}\Big] - \sum_{n=1}^{4}\frac{\alpha_n}{n!}\,\phi_0^n\,. \tag{46}$$

The counterterms appear as a quartic polynomial in ϕ_0, and the (infinite) coefficients α_n are determined by specifying appropriate renormalization conditions on the energy. Following refs. 57 and 7, we will choose the counterterms to cancel the first four powers of ϕ_0 appearing in the expansion of the infinite sum over energies. Although this procedure is not unique, it has the virtue of minimizing the many-body forces arising from this vacuum correction, and it is easy to verify that only the first four terms in this expansion produce divergent results. The divergences can be defined by converting the sum to an integral and then regularizing dimensionally.[63]

After removing the divergences with the counterterms, the remaining terms are finite, and one finds

$$\Delta\mathcal{E}(M^*) = -\frac{1}{4\pi^2}\Big\{M^{*4}\ln(M^*/M) + M^3(M-M^*) - \frac{7}{2}M^2(M-M^*)^2 + \frac{13}{3}M(M-M^*)^3 - \frac{25}{12}(M-M^*)^4\Big\}\,. \tag{47}$$

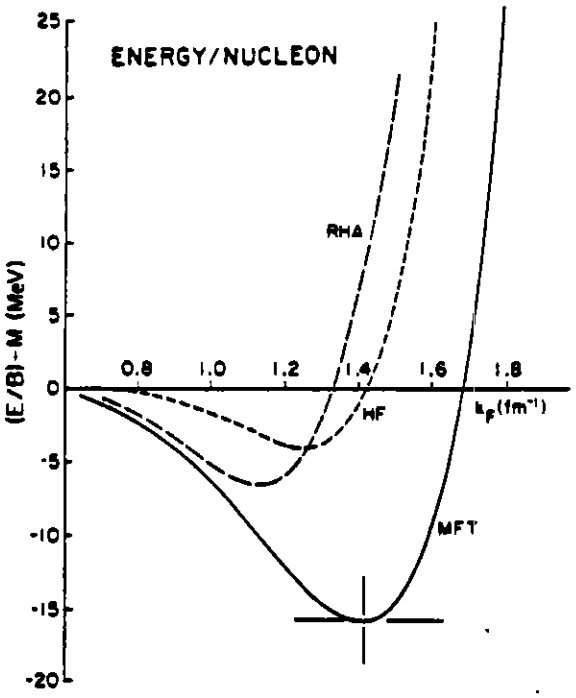

Figure 12: Energy/nucleon in nuclear matter. The mean-field theory (MFT) results are shown as a solid line. The relativistic Hartree approximation (RHA), which includes the one-loop vacuum correction, produces the long-dashed line, while the short-dashed line is from a relativistic Hartree–Fock calculation (discussed below). All results are computed with parameter set L1 in table 1.

Just as in the MFT, $M^* \equiv M - g_s\phi_0$ is determined at each ρ_B by minimization, which produces the one-loop (RHA) self-consistency condition [compare eq. (20)]

$$M^* = M - \frac{g_s^2}{m_s^2}\frac{\gamma}{(2\pi)^3}\int_0^{k_F} \mathrm{d}^3k\, \frac{M^*}{E^*(k)} + \frac{g_s^2}{m_s^2}\frac{1}{\pi^2}\left\{M^{*3}\ln(M^*/M) - M^2(M^*-M) - \frac{5}{2}M(M^*-M)^2 - \frac{11}{6}(M^*-M)^3\right\}. \quad (48)$$

Note that the solution to this equation contains all orders in the coupling g_s.

Although $\Delta\mathcal{E}$ has historically been called the "vacuum fluctuation correction," this appellation is somewhat unfortunate, since it does not involve any fluctuations. More precisely, $\Delta\mathcal{E}$ is the finite shift in the baryon zero-point energy that occurs at finite density, and is analogous to the "Casimir energy" that arises in quantum electrodynamics. We emphasize that the zero-point (one-loop) vacuum correction is insensitive to the short-distance structure of the baryons, as it arises solely from the change in the baryon mass in the presence of the *uniform* scalar field ϕ_0.[c]

To discuss the size of the one-loop vacuum correction, we can compare predicted quantities using a *fixed* set of parameters determined from the empirical saturation

[c]In addition, this correction cannot be calculated in nonrenormalizable meson–baryon models that are regularized by inserting *ad hoc* form factors at the meson–baryon vertices, since the uniform scalar field involves only zero-momentum-transfer components of the interaction between baryons, and the usual form factors have no effect on these contributions.

properties of nuclear matter in the MFT. (Alternatively, one could compare results after determining a separate set of RHA parameters that reproduce nuclear matter saturation.) Figure 12 shows the energy/nucleon for the MFT and RHA approximations. Observe that the equilibrium Fermi wavenumber k_F^0 shifts by roughly 0.25 fm^{-1}, and the binding energy decreases by about 10 MeV when the one-loop vacuum correction is included. Although the latter is small on the scale of the large scalar and vector fields, the modification to the binding energy is significant, reflecting the sensitive cancellation between the attractive and repulsive components in the potential energy. The one-loop vacuum corrections are a direct consequence of the relativistic treatment of the nuclear many-body problem and are absent in a nonrelativistic approach.

In a finite nucleus, the zero-point corrections to the Dirac–Hartree hamiltonian (and the resulting energy functional) arise in just the same way as in eq. (13). The sum over the negative-energy eigenvalues [which augments eq. (36)] must now be computed using the spectrum of eq. (24), and both bound and continuum states are to be included. Since the eigenvalues cannot be determined in closed form due to the spatial dependence of the meson fields, the calculation is considerably more complicated than for nuclear matter. Nevertheless, the corrections have been computed essentially exactly, by starting with a local-density approximation[64] and then by systematically adding corrections from gradients of the meson fields.[65–69]

If the model parameters are adjusted from their previous values to reproduce the desired nuclear matter properties[(d)] when the zero-point corrections are added to the infinite nuclear matter energy density, the resulting parameters[68] are given in the row labeled RHA0 in table 1. The nuclear matter compressibility decreases to $K \approx 452$ MeV, and the baryon effective mass at equilibrium is $M^*/M \approx 0.73$. How do the additional zero-point corrections change the systematic description of nuclear properties? Since the nuclear compressibility is still rather high, the calculated nuclei remain slightly underbound and the surface thicknesses are too small.[68] The increased M^* leads to a slightly more compressed spectrum of states near the Fermi surface (in heavy nuclei) and a smaller spin-orbit force. Thus, although predicted nuclear deformations still follow the correct systematics,[52] the spin-orbit splittings are too small by about 50%.[68] The shell oscillations in the nuclear interior are essentially unchanged. The derivative contributions to the local-density approximation are not negligible, but they generate only small changes in nuclear properties once the parameters are re-fitted to the standard input data. We conclude, therefore, that although the zero-point corrections give non-negligible corrections to the simple mean-field results, they do not improve the nuclear systematics.

The Relationship Between QHD and QCD

There is by now overwhelming evidence that hadrons are themselves composed of

[(d)] We enforce equilibrium at $k_F = 1.30\,\text{fm}^{-1}$ with a binding energy of 15.75 MeV and a symmetry energy of 35 MeV. The scalar mass is again chosen to reproduce the observed rms radius of ^{40}Ca.

quarks and gluons. It is also widely believed that the quark-gluon dynamics is described by the nonabelian gauge theory of quantum chromodynamics. A discussion of the QCD lagrangian is beyond the scope of this talk, but this theory is presented in several texts (see, for example, Huang[70] or Rivers[71]), and a brief introduction is given in ref. 7. Quantitative QCD predictions at length scales relevant for hadronic and nuclear phenomena (which would specify precisely the relationship between QCD and QHD) are exceedingly difficult and are currently being pursued at the forefront of relativistic many-body theory. Here we will simply illustrate a simple model calculation of the phase diagram for nuclear matter, where the hadronic phase is described by the MFT of QHD–I, and the quark-gluon phase is described by QCD. This model contains a first-order transition between the hadronic and quark-gluon phases. Although there are some indications from recent QCD lattice simulations that there is no first-order phase transition at zero density for two quark flavors,[72] the nature of the transition at finite density is unknown. Thus a simple two-phase model may still provide a reasonable first approximation to the nuclear equation of state at all temperatures and finite densities.

Our previous discussion of the hadronic equation of state was restricted to zero temperature. The extension to finite temperature is straightforward in the MFT, since the hamiltonian is diagonal and the mean-field thermodynamic potential Ω can be calculated exactly.[(e)] The results for the scalar density, baryon density, energy density, and pressure are given by[7]

$$\rho_s = \frac{\gamma}{(2\pi)^3}\int \mathrm{d}^3k\,\frac{M^*}{E^*(k)}(n_k+\bar{n}_k)\,, \tag{49}$$

$$\rho_B = \frac{\gamma}{(2\pi)^3}\int \mathrm{d}^3k\,(n_k-\bar{n}_k)\,, \tag{50}$$

$$\mathcal{E} = \frac{g_v^2}{2m_v^2}\rho_B^2 + \frac{m_s^2}{2g_s^2}(M-M^*)^2 + \frac{\gamma}{(2\pi)^3}\int \mathrm{d}^3k\,E^*(k)(n_k+\bar{n}_k)\,, \tag{51}$$

$$p = \frac{g_v^2}{2m_v^2}\rho_B^2 - \frac{m_s^2}{2g_s^2}(M-M^*)^2 + \frac{1}{3}\frac{\gamma}{(2\pi)^3}\int \mathrm{d}^3k\,\frac{\mathbf{k}^2}{E^*(k)}(n_k+\bar{n}_k)\,, \tag{52}$$

where the baryon and antibaryon distribution functions are

$$n_k(T,\nu) \equiv \frac{1}{1+\mathrm{e}^{[E^*(k)-\nu]/T}}\,, \quad \bar{n}_k(T,\nu) \equiv \frac{1}{1+\mathrm{e}^{[E^*(k)+\nu]/T}}\,, \tag{53}$$

and the reduced chemical potential is $\nu \equiv \mu - g_v V_0$. (We set Boltzmann's constant $k_B = 1$.) The nuclear matter equation of state at all densities and temperatures for this hadronic MFT model (QHD–I) is shown in fig. 13.

Figure 14 shows the self-consistent nucleon mass obtained my minimizing eq. (51) with respect to M^*. The striking feature is the sudden decrease of the nucleon mass well below $T = M$. Thus, at high temperature (as at high density), the baryons are essentially massless.

[(e)] We neglect the zero-point corrections from the Dirac sea in this section (see refs. 32 and 73), as well as thermal contributions from the massive isoscalar mesons.

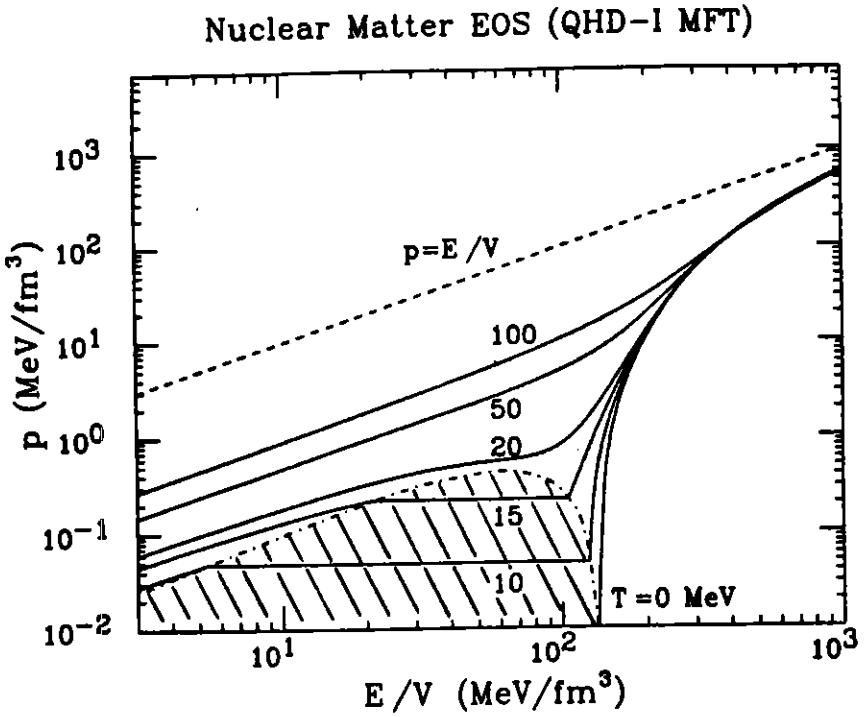

Figure 13: Nuclear matter equation of state on isotherms. The dashed line represents the causal limit, and the shaded area shows the region of phase separation, as determined by a Maxwell construction. The solid curves are labeled by the temperature, in MeV, and the critical temperature is approximately 18.3 MeV. Here the parameter set L2 is used.

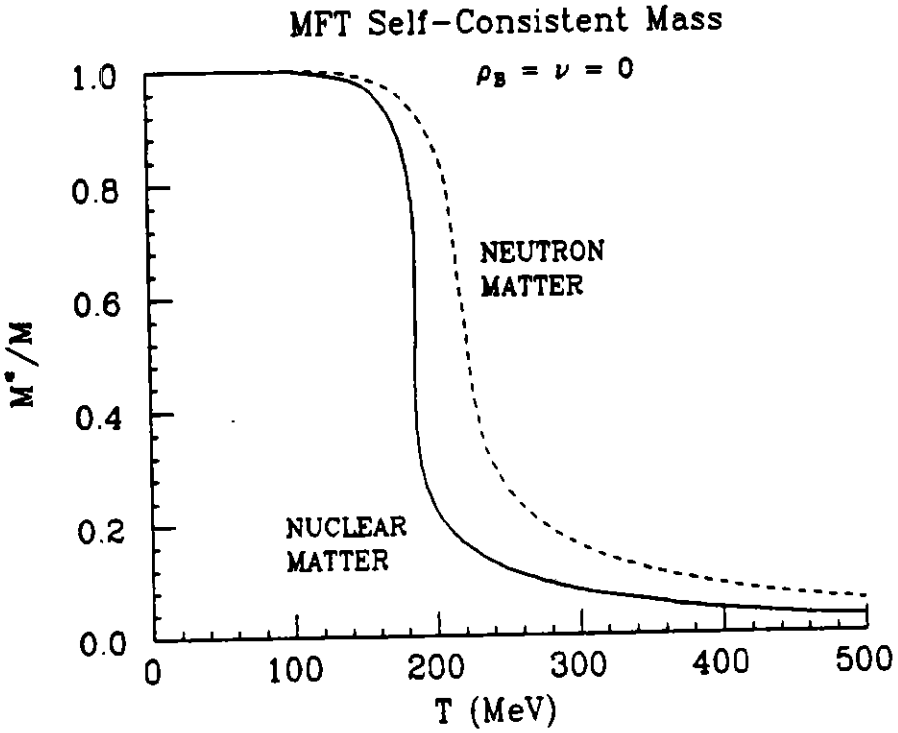

Figure 14: Self-consistent nucleon mass as a function of temperature at zero baryon density. The value of M^*/M is 0.5 for $T \approx 186$ MeV and $T \approx 222$ MeV in nuclear and neutron matter, respectively. Parameter set L2 is used.

For the quark phase, we use a simple model based on QCD and its properties of *asymptotic freedom* and *confinement*. Asymptotic freedom implies that when all of the momenta in a process are large, the renormalized coupling constant for that process becomes small, while confinement reflects the empirical fact that free quarks and gluons are never observed in the laboratory. We limit ourselves to the "nuclear domain," where only u and d quarks are important, and these quarks are assumed to be massless. Since the quark-gluon phase will be relevant only at extremely high temperatures or densities, where the particles have large momenta, we neglect interactions between the quarks except for a constant, positive energy/volume in the vacuum $(E/V)_{\rm vac} = b$, which models the confinement dynamics. This constant can be interpreted as the energy needed to create a bubble or bag in the vacuum, in which the noninteracting quarks and gluons are confined.

With this model, the QCD equation of state takes the simple form[74]

$$p = \tfrac{1}{3}(\mathcal{E} - 4b) \tag{54}$$

for both nuclear and neutron matter *at all densities and temperatures*. The "bag parameter" b determines the density of the hadron–quark phase transition, and since it represents a bulk property of nuclear systems, it may be different from values determined from the static properties of hadrons. The parameter b is constrained by requiring that at zero temperature and nuclear equilibrium density, the favored phase is the hadronic phase. Here we use $b = 131.2\,\mathrm{MeV/fm^3}$, taken from ref. 7, where it is shown that this value is consistent with the above requirement.

Figure 15 shows the resulting curves for this two-phase model of nuclear matter. The hadronic segments are determined from eqs. (51) and (52), together with the couplings and masses from row L2 in table 1. The quark-gluon curve is calculated from eq. (54), and Gibbs' criteria for phase equilibrium ($\mu_1 = \mu_2$, $p_1 = p_2$, $T =$ constant) are used to deduce the region of phase coexistence arising from the first-order transition. The complete phase diagram of nuclear matter is described by a one-parameter model, which allows for a simple correlation of phenomena occurring in very different regimes of the thermodynamic variables. Note that at high enough baryon density or temperature, *one always produces the quark-gluon phase* with an equation of state given by eq. (54).

Although this model is very simple, it has several nontrivial features. First, it is based on a completely relativistic calculation of the nuclear matter phase diagram and phase transition. Second, the statistical mechanics has been done exactly at all temperatures and densities. Third, the QHD model of the hadronic phase successfully describes many bulk properties of nuclear matter and finite nuclei. Fourth, the QCD phase obeys asymptotic freedom.

Finally, the model can be improved by systematically including additional mesonic degrees of freedom (such as thermally excited pions) and by going beyond the mean-field approximation for the hadronic phase. Interactions can also be included in the quark-gluon phase to calculate the corrections to the asymptotically free equation of state. At vanishing density, these corrections can be computed using the techniques of

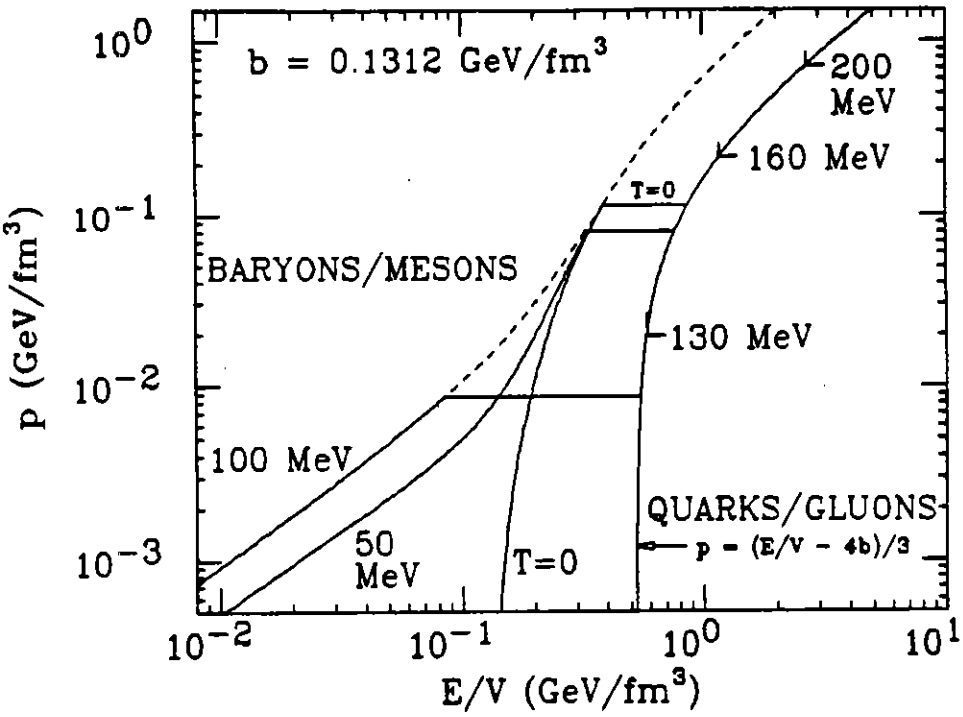

Figure 15: Equation of state isotherms for nuclear matter for the indicated values of the temperature. Phase equilibrium exists along the horizontal segments, which are determined by a Maxwell construction. The left-hand endpoints of the higher-temperature curves correspond to zero baryon density.

lattice gauge theory, as summarized by Gottlieb.[72] Lattice calculations, however, are not currently practical at finite density, although alternative nonperturbative techniques have been developed for hot QCD.[75,76]

EXTENSIONS AND ISSUES

We have seen that the mean-field approximation to QHD gives a concise and highly successful nuclear phenomenology. In QHD, however, one can in *principle* go beyond the MFT, calculate to arbitrary accuracy, and then compare with experiment. In *practice* this program is extremely difficult, since QHD is a strong-coupling relativistic quantum field theory.[f] Nevertheless, the Feynman rules for the Green's functions are well defined. Thus, just as in nonrelativistic many-body theory, one can use intuition to sum selected infinite sets of diagrams, determine the renormalized coupling constants by refitting nuclear matter properties, and then see whether the MFT results are *stable* under the inclusion of these additional contributions, while investigating new physical phenomena. Many such applications are discussed in ref. 7, where the historical development is presented. This 1986 volume is updated in ref. 77. It is impossible to review all that material and to give an exhaustive list of recent references here. We shall instead present some selected results of extensions beyond the MFT and discuss

[f]Indeed, a theory that is not asymptotically free.

some of the issues raised by this work.

All of the extensions we discuss involve loop corrections to the MFT of one sort or another. In the MFT, the baryon Green's function can be written as[7]

$$G(k) = (\gamma_\mu k^{*\mu} + M^*)\left\{\frac{1}{k^{*2} - M^{*2} + i\epsilon} + \frac{i\pi}{E^*(k)}\delta[k_0^* - E^*(k)]\theta(k_F - |\mathbf{k}|)\right\}$$
$$\equiv G_F(k) + G_D(k)\ , \tag{55}$$

where $k^{*\mu} \equiv (k^0 - g_v V_0, \mathbf{k})$ is the kinetic four-momentum[g] and $E^*(k) = \sqrt{\mathbf{k}^2 + M^{*2}}$. The first term $G_F(k)$ is the Feynman propagator for a baryon of mass M^*, and the second term is the contribution arising from baryons already present at finite density; this latter contribution reproduces the MFT results. In discussing the following extensions, we shall frequently distinguish between results obtained with the full baryon propagator $G(k)$ and with just the second, or "density-dependent," contribution $G_D(k)$. Since the three- and four-momenta are constrained in $G_D(k)$, loop integrals over this second term give well-defined, finite results that are direct analogues of the terms arising in nonrelativistic many-body theory.

Relativistic Hartree–Fock

Relativistic Hartree theory is obtained by self-consistently summing the tadpole graphs in the baryon self-energy. Retention of G_D in the tadpoles gives rise to the MFT, while the full G with appropriate counterterms $\delta\mathcal{L}$ produces the RHA, as discussed in the previous section. A characteristic result of QHD–I is that the Lorentz scalar and vector self-energies are very large; these contributions *cancel* in the binding energy but *add* in the spin-orbit interaction. Hartree–Fock (HF) theory is obtained by including the meson emission and reabsorption ("exchange") graphs in the baryon proper self-energy. A calculation of these graphs[78] with G_D for nuclear matter and the coupling constants L1 from table 1 produces the results shown in figs. 12 and 16. Some conclusions from this work are as follows:

1. These HF calculations give exchange terms that are the direct relativistic generalization of those arising when Slater determinants are used to find the best single-particle wave functions in nonrelativistic many-body theory.

2. Once the large scalar and vector self-energies have been established in relativistic Hartree theory, the inclusion of the exchange terms does not qualitatively alter the results.

3. The MFT is thus *stable* under the inclusion of the exchange contributions. In fact, after refitting to the equilibrium nuclear matter properties, the binding energy curves in relativistic Hartree and Hartree–Fock are almost indistinguishable.[7]

[g] Note that in closed-loop integrals, such as those involved in computing the ground-state energy, a simple shift of integration variables allows one to eliminate the dependence on $g_v V_0$.

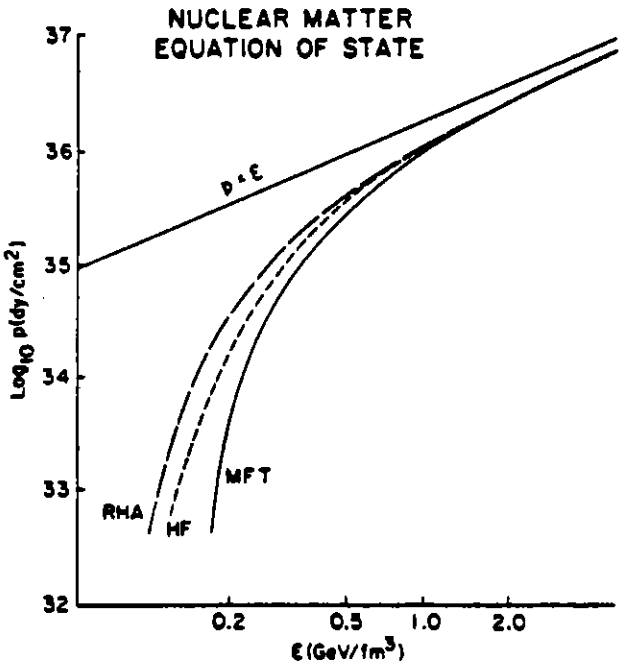

Figure 16: Nuclear matter equation of state at zero temperature.[7] The curves are labeled as in fig. 12.

4. The HF equation of state approaches that of the MFT at high baryon density.

5. The fully self-consistent Hartree–Fock theory that retains the complete $G(k)$ and meson retardation is complicated;[79] it has not yet been successfully solved.

Relativistic Brueckner–Bethe–Goldstone

In nonrelativistic nuclear many-body theory, the two-nucleon potential V is strong and singular; it has a hard core at short distances. It is therefore necessary to solve for the correlated two-nucleon wave function in the medium. This Bethe–Goldstone wave function vanishes at the core radius and *heals* to the unperturbed wave function at large distances.[(h)] The product $V\psi$ is thus well defined and leads to a finite energy shift. In QHD–I, however, the interaction is integrable, so that results are sensible even at the mean-field level. The saturation of nuclear matter arises at this level from the saturation of the scalar attraction with increasing density. This scalar attraction is equivalent to an infinite series of velocity-dependent interactions in the nonrelativistic language. It is of interest to see if the MFT results are stable with respect to the inclusion of two-body correlations; in diagrammatic terminology, this amounts to summing the ladder diagrams for the baryon proper self-energy. Several relativistic calculations of this type

[(h)]The vanishing wave function at short distance implies an insensitivity to what is going on inside the hard-core radius. This insensitivity is responsible for much of the success of nonrelativistic nuclear physics.

have been carried out for nuclear matter.[80-82] Some observations, conclusions, and issues are as follows:[80]

1. The box diagram that forms the fundamental unit of the ladder sum involves a loop integration.

2. There are many possible reductions of the relativistic, four-dimensional Bethe–Salpeter equation in the medium to a unitary, three-dimensional integral equation that can be identified as the relativistic extension of the Bethe–Goldstone equation. Numerical results for the binding energy are sensitive to the reduction used.

3. Even after this reduction, calculated results are sensitive to the high-momentum part of the loop integrals, implying important contributions from baryon transitions to states lying well above the Fermi surface. Phenomenological form factors significantly reduce this sensitivity.

4. Since M^* enters in both the positive- and negative-frequency Dirac spinors, the binding energy of nuclear matter is sensitive to the self-consistency condition. At present, it is not known how to construct a self-consistency condition that leads to a conserving approximation when relativistic ladder diagrams are included.

5. Although the shifts in the binding energy of nuclear matter are large, the MFT is again stable with respect to the inclusion of two-baryon correlations on the scale of the large scalar and vector self-energies of the MFT.

6. The equation of state of nuclear matter again becomes the MFT result at high baryon density.

7. For free NN scattering, the corresponding calculation in QHD–I gives results in qualitative agreement with observation, but the charged isovector π and ρ mesons must be included to achieve a quantitative description.[80,82]

8. The fully relativistic Bethe–Salpeter equation in nuclear matter remains to be investigated.

9. In view of the above issues, a quantitative calculation of the binding energy of nuclear matter in QHD is not possible at this stage of the development.

Relativistic Random-Phase Approximation (RRPA)

The sum of fermion ring diagrams gives the correct high-density limit for the correlation energy in the electron gas, where the Coulomb interaction is $e^2/\mathbf{q}^2$.[(i)] One might hope that the corresponding sum of baryon ring diagrams gives the correct high-density correlation energy in QHD–I, when the dimensionless meson masses m^2/k_F^2

[(i)] For the present purposes, the sum of rings is equivalent to the random-phase approximation (RPA).

become small. The sum of the ring diagrams for nuclear matter in QHD–I was first investigated by Chin.[57] Applications to the spectra of finite nuclei were initiated by Furnstahl,[58,83] and there has been a great deal of recent activity in this area.[84–91,60] We shall refer to the calculation of the rings that keeps only terms with at least one factor of G_D as the RPA; this calculation includes loops at least linear in the density and is the direct relativistic extension of the RPA in nonrelativistic many-body theory. The calculation that also includes the modification of the strong vacuum polarization in the nuclear medium due to the shift $M \to M^*$ will be called RRPA. Some results of this work and issues raised by it are the following:

1. The scalar and vector propagators mix in nuclear matter. Chin showed that at high density, vector meson exchange dominates in QHD–I. The excitation spectrum of nuclear matter in the RPA is that of zero sound, and the sound velocity c_0 approaches the speed of light from below as the baryon density gets large ($c_0 \to 1^-$ as $k_F \to \infty$). This implies that signals in the medium cannot propagate faster than the speed of light, in accord with special relativity. There are other branches in the excitation spectrum corresponding to meson propagation.

2. In nuclear matter in the RRPA, poles appear in the polarization propagator at zero frequency $q_0 = 0$ and finite wavenumber $|\mathbf{q}| \neq 0$; the value of this wavenumber is a few times the nucleon mass in QHD–I.[57,84–86,91] Such poles imply an instability of the system against density fluctuations of the corresponding wavelength. There are several possible interpretations of these results:

   (a) The RRPA for the propagators is inadequate.

   (b) Vertex modifications are important. (Phenomenological form factors affect the numerical results significantly.[84])

   (c) The composite structure of the baryon must be taken into account before one reaches distance scales where these poles develop.

   (d) The instability is real.

3. The polarization propagator governs the linear response of the system. The calculated isoscalar linear response in QHD–I leads to a reduction of the Coulomb sum rule.[87–90,60] There is roughly a 15% reduction in the RPA and an additional 15% reduction in the RRPA.[87] The observed experimental reduction of the Coulomb sum rule is one of the outstanding unsolved problems in traditional nonrelativistic nuclear physics.

4. In finite nuclei, it is essential to admix negative-frequency baryon components into the wave functions to bring the spurious $(1^-, 0)$ state down to zero frequency, to maintain current conservation, and to produce nuclear isoscalar magnetic moments that agree with the Schmidt lines.[61,92]

5. The RRPA calculation involves loop integrations and strong vacuum polarization. Physical effects come from the *modification* of these processes in the nuclear

medium. The calculation of hadronic contributions to strong vacuum polarization is a central problem in QHD. More generally, at some distance scale, this vacuum polarization should be calculated in terms of quarks and gluons.

The Quantum Vacuum

One goal in QHD is to systematically calculate the vacuum-loop corrections to the MFT. The one-loop correction from G_F produces the RHA, and we have seen that the MFT is stable against the one-loop vacuum contributions. A path-integral representation of the generating functional shows that the loop expansion is in $\hbar$, with the one-loop contribution the first quantum correction about the classical path of stationary action. One might hope that the two-loop correction would be the next term in a converging expansion. The calculation of the two-loop contribution to the properties of nuclear matter is nontrivial; it is carried out for QHD-I in ref. 12. (See also refs. 77 and 93.) The basic conclusion from this analysis is the following: although formally an expansion in $\hbar$, the parameters characterizing the loop contributions to the properties of nuclear matter are: (i) dimensionless coupling constants $(g_v^2/4\pi\hbar c, g_s^2/4\pi\hbar c^3)$, (ii) lengths $(\hbar/m_v c, \hbar/m_s c, \hbar/Mc, 1/k_F)$, and (iii) energies $(m_v c^2, m_s c^2, Mc^2, \hbar c k_F)$. The loop expansion is essentially an expansion in the dimensionless coupling constants, which are large in QHD. The quantum corrections are correspondingly large, the series is not converging, and the MFT *is not stable against this perturbative loop expansion.* Clearly, an alternative procedure must be found to systematically and reliably calculate vacuum corrections to the MFT results in QHD.

The computation of hadronic contributions to vacuum polarization is a central issue in QHD, and more generally, in all of physics. There *are* indeed hadronic contributions to vacuum polarization; for example, a spectral analysis of the strong-interaction contribution to electromagnetic vacuum polarization shows that the spectral weight function starts at $4m_\pi^2$:[j]

$$\Pi^{str}_{\mu\nu}(q) = (q_\mu q_\nu - q^2 g_{\mu\nu})\Pi(q^2) \ ,$$

$$\Pi(q^2) = \frac{1}{\pi}\int_{4m_\pi^2}^{\infty} \frac{\rho(\sigma^2)}{\sigma^2 - q^2}\, d\sigma^2 \ . \qquad (56)$$

In the complex q^2 plane, $\Pi(q^2)$ is an analytic function with a branch cut running along the real axis from $4m_\pi^2$ to ∞. The discontinuity across that cut for $4m_\pi^2 \le q^2 \le 9m_\pi^2$ comes from the electroproduction of two real pions. Thus the low-mass singularities of propagator and vertex functions are most efficiently expressed in terms of hadronic variables.

The contribution of two pions to vacuum polarization at all q^2 can be calculated in QHD-II; it will be well defined and finite. (Vertex modifications will exist in QHD-II

[j] Pions are included in QHD-II; we use this as the simplest example for the present discussion.

and can also be included.) The result will not be meaningful if the dominant contribution to the loop integration comes from very high momenta and short distances, since there a QHD description is clearly wrong.[k] In this instance, one *must* invoke quarks, gluons, and QCD. At short-enough distances, one can use perturbative QCD. On the other hand, at low momenta and long distances, for example, in the low-mass part of the spectral function, QCD is a strong-coupling theory and the effective degrees of freedom are the hadrons, in this case, two pions. Hopefully, once vertex corrections are included, QHD has the possibility of describing the low-lying hadronic contributions to the spectral weight function and vacuum polarization.

The Vertex

As mentioned earlier, vector meson exchange dominates at high baryon density in QHD–I, where the vector meson is coupled to the conserved baryon current. Milana[94] observes that in a theory with vector coupling, the vertex form factor is a decreasing function of q^2. This implies a decreased sensitivity to the high-momentum or short-distance contributions to loop integrals and would provide a favorable situation for QHD. It is essential to include vertex corrections in QHD to determine its full implications.[l] The fully off-shell vertex is complicated in any field theory. Reference 94 is the only vertex study in QHD of which the present authors are aware.

Pions and Chiral Symmetry

The relativistic neutral scalar and vector fields are the most important for determining the bulk properties of nuclear systems. Nevertheless, the lightest and most accessible meson is the pion, whose interactions with nucleons and nuclei have been extensively studied at the meson factories. It is therefore impossible to formulate a complete and quantitative hadronic theory without including pionic degrees of freedom.

Pion interactions are constrained by the observed, nearly exact, SU(2) isospin symmetry. In addition, the soft-pion theorems, the partial conservation of the axial current (PCAC) in weak interactions, and the theory of QCD indicate that pion dynamics is also constrained by *chiral* symmetry, which enlarges the symmetry group from SU(2) to $\mathrm{SU}(2)_L \times \mathrm{SU}(2)_R$. Here "$L$" and "$R$" denote left- and right-handed isospin rotations, respectively. A thorough discussion of chiral symmetry is beyond the scope of this talk, but we note that this symmetry has important consequences for the way mesons interact with themselves, as we will discuss shortly.

Pions can be included in a chiral-invariant manner using the linear σ model.[22–24] This model contains a pseudoscalar coupling between pions and nucleons and an auxiliary scalar field σ to implement the chiral symmetry.[m] Weinberg's transformation[95] can

[k] Moreover, for large σ^2 in eq. (56), the two-pion intermediate state by itself is inadequate.

[l] These vertex corrections reflect the internal hadron structure present in QHD.

[m] The presence of an isoscalar vector field V^μ coupled to the baryon current with minimal coupling

then be used to transform to a pseudovector (derivative) πN coupling multiplied by an infinite series of nonlinear pion terms. There are two advantages to this transformation: first, the decoupling of pions as $q_\lambda \to 0$ is now explicit (as are the soft-pion theorems), and second, the new pseudovector coupling constant is

$$f^2 = g_\pi^2 \left(\frac{m_\pi}{2M}\right)^2 \approx 1.0 \; . \tag{57}$$

This is much smaller than the pseudoscalar coupling constant $g_\pi^2/4\pi \approx 14.4$.

In the limit that the chiral σ mass $m_\sigma \to \infty$, the auxiliary scalar field decouples, and what remains for the pions and baryons is the nonlinear σ model of Weinberg.[95] For any finite value of m_σ, however, the theory is renormalizable, and it can be used to calculate nuclear pion processes.[21,96]

Nevertheless, there is a serious problem here.[7] Suppose the auxiliary scalar field σ in the chiral-invariant linear σ model is identified with the low-mass scalar field ϕ in QHD–I. Then the nonlinear meson couplings ($\phi^3, \phi^4, \phi^2\pi^2$) that remain after spontaneous symmetry breaking are so strong that they preclude a successful MFT of nuclear matter and finite nuclei.[97,21] Equivalently, nonlinear many-body forces are implied that are difficult to reconcile with what is known about nuclear physics.

A possible resolution of this problem is that the chiral σ mass m_σ is very large, reducing the effects of the nonlinear couplings, and that the low-mass scalar field ϕ in QHD–I is generated *dynamically* through the couplings of the chiral σ and the pions. In ref. 98, the process $\pi + \pi \to \pi + \pi$ is investigated within the framework of the σ model with a high mass σ. The chiral-invariant Born amplitude is unitarized, and the resulting phase shift in the $(0^+, 0)$ channel is shown in fig. 17. One observes a broad, low-mass, near-resonant amplitude in this channel, even though the chiral σ has a large mass.

When this model $\pi\pi$ scattering amplitude is included in the two-pion-exchange part of the NN interaction (see fig. 18), the result is a dynamically generated, broad, low-mass ($\approx$ 600 MeV) peak that resembles the exchange of a light scalar meson. This peak arises even when the *chiral* scalar field has a large mass ($m_\sigma \approx 10$ GeV). It is further demonstrated in ref. 98, within the framework of the linear σ model, that this $(0^+, 0)$ channel leads to the observed intermediate-range attraction in the NN force.

The evident role of the low-mass scalar meson channel in nuclear physics can therefore be understood within the framework of chiral symmetry. The importance of the resulting scalar-isoscalar mean field and optical potential in producing a successful nuclear phenomenology was illustrated in the preceding section. Note, however, that the representation of this effective hadronic degree of freedom through the ϕ field in the local relativistic quantum field theory of QHD–I is a much more sweeping assumption.

For the pion-nucleon interaction, one is left with the nonlinear σ model of Weinberg: derivative couplings to baryons multiplied by $[1 + (f/m_\pi)^2\pi^2]^{-1}$. In the end, one has a chirally invariant theory including pions that reproduces the soft-pion theorems, that

affects none of these arguments.

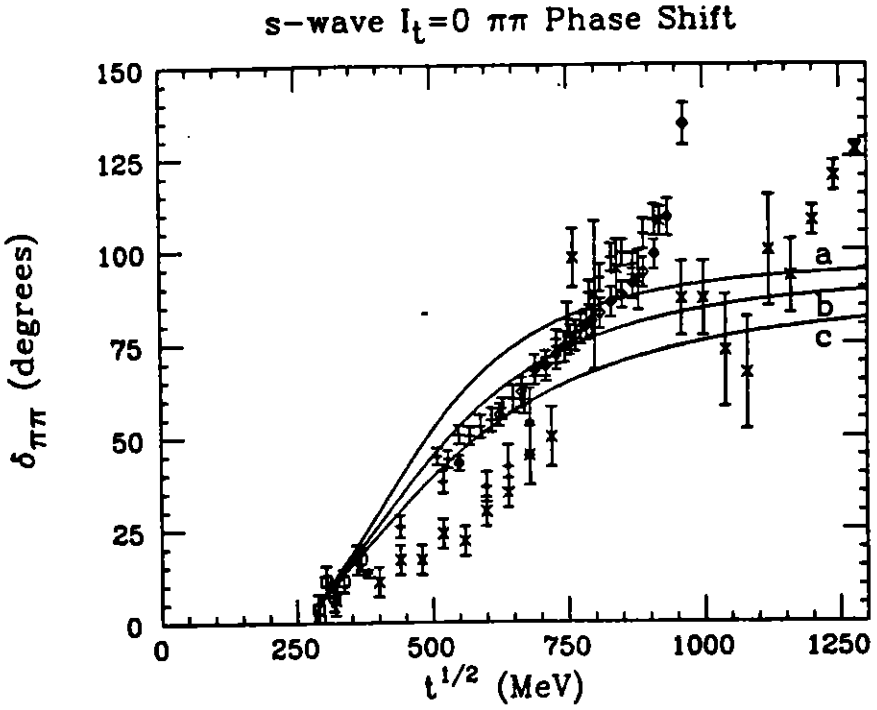

Figure 17: The s-wave isoscalar $\pi\pi$ phase shift as a function of the total cm energy.[98] The chiral σ masses used here are (a) $m_\sigma = 950$ MeV, (b) 1400 MeV, and (c) 14 GeV.

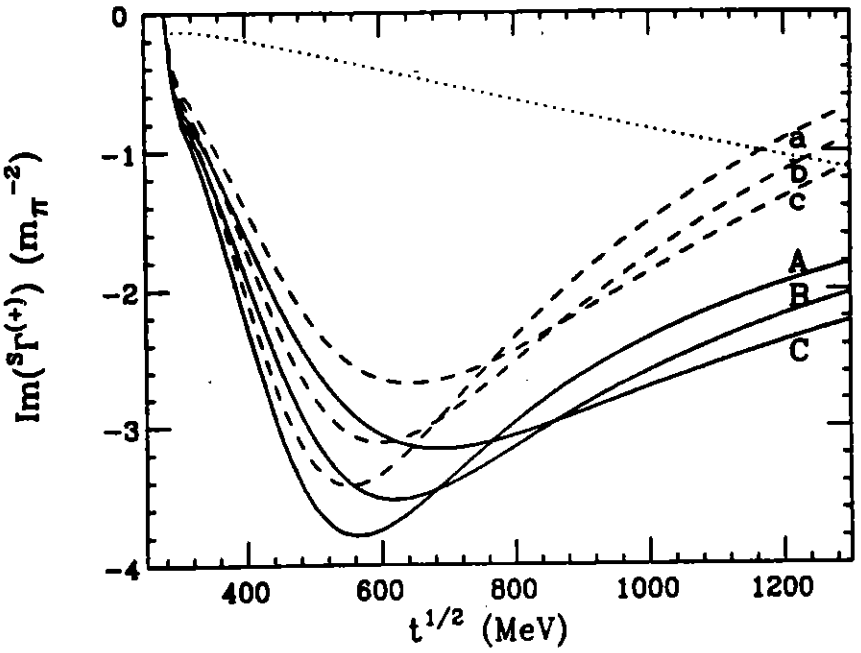

Figure 18: The spectral weight function for the NN interaction in the scalar-isoscalar channel, from ref. 98. Note that the interaction is attractive. The solid (dashed) curves give the result before (after) the subtraction of the iterated two-pion-exchange box diagram. The chiral mass is $m_\sigma = 950$ MeV, 1400 MeV, and 14 GeV for the curves labeled A (a), B (b), and C (c).

produces a low-mass effective scalar meson dynamically, and that is renormalizable for any large but finite m_σ.

The ρ can be included in this renormalizable theory by starting with a nonabelian Yang–Mills theory based on isospin and then using spontaneous symmetry breaking and the Higgs mechanism to generate the ρ mass, as in the standard model of electroweak interactions. The resulting theory QHD–II, with σ, ω, π, and ρ mesons, is discussed more fully in ref. 7.

Hadronic Degrees of Freedom

The essential phenomenological features of the low-energy πN interaction are that low-momentum pions interact weakly with nucleons (they decouple as $q_\lambda \to 0$) and that the interaction is dominated by the first pion-nucleon resonance, the $\Delta(1232)$. This resonance represents the first excited state of the baryon, with $(J^\pi, T) = (\frac{3}{2}^+, \frac{3}{2})$. It is essential to have this degree of freedom in the theory, or the results will look nothing like nuclear physics. It is impossible to put a field with these quantum numbers into a simple renormalizable lagrangian. Thus the hope is that this degree of freedom, as with the low-mass scalar field, is again produced *dynamically* within the model. Fortunately, as has been shown in ref. 99, this is indeed the case.

In ref. 99, the sum of πN ladder diagrams with nucleon exchange is investigated within the framework of the chiral πN theory discussed above. Partial-wave dispersion relations are used, the one-baryon-exchange mechanism is input as the driving term, and the resulting integral equations are solved with the N/D method. This is a relativistic extension of nonrelativistic Chew–Low theory. As with Chew–Low, a resonance is found in the $(\frac{3}{2}^+, \frac{3}{2})$ channel.

The box diagram in the ladder sum involves a loop integral, which is finite and well defined in this renormalizable theory. Nevertheless, the loop integration involves significant contributions from high momenta or short distances, and thus the *position* of the resonance is sensitive to the approximations made; the *width* is much less so.[n] It is clear, however, that the first excited state of the nucleon, the $\Delta(1232)$ with $(\frac{3}{2}^+, \frac{3}{2})$, which is the dominant feature of low-energy pion-nucleus interactions, can be generated *dynamically* in QHD.

Other baryon properties arise through different loop integrals in QHD. For example, the vertex diagram consisting of the emission of a pion, its interaction with the virtual electromagnetic field, and its reabsorption by the nucleon contributes to the nucleon's anomalous magnetic moment. The two-pion contribution gives the low-mass, or long-distance, part of the spectral weight function for the anomalous magnetic form factor $F_2(q^2)$:

$$F_2(q^2) = \frac{1}{\pi} \int_{4m_\pi^2}^{\infty} \frac{\rho_2(\sigma^2)}{\sigma^2 - q^2} \, \mathrm{d}\sigma^2 \ . \tag{58}$$

[n] Vertex corrections will again modify this sensitivity to the high-momentum behavior.

Assume that the two-pion contribution arising from this vertex diagram dominates the spectral weight function everywhere. One then gets a semi-quantitative account of the isovector anomalous magnetic moment and its mean square radius.[7(o)]

A few comments are relevant here:

1. The dynamical model of ref. 99 allows for the investigation of many interesting questions concerning the behavior of the Δ in the many-body nuclear system, for example, its binding energy in nuclear matter, its optical potential, and the modification of its electroweak properties in the nuclear medium.

2. The production of effective degrees of freedom through dynamical means in QHD, as for the low-mass scalar field with $(0^+, 0)$ and the first excited state of the baryon with $(\frac{3}{2}^+, \frac{3}{2})$, while gratifying, also raises serious issues:

   (a) When does one stop? It is apparently necessary to investigate all possible hadronic channels for resonant behavior; there will be many such resonances.

   (b) Which of these resonances must be included as dynamical input in the generation of others?[(p)]

   (c) And, a more serious question, which of these hadrons are to be included through local fields in a QHD lagrangian density?

   (d) It is only a hope that one can get a self-contained dynamical description of nuclear physics in the low-energy hadronic sector with a few judiciously chosen hadronic degrees of freedom and a local, relativistic, renormalizable quantum field theory based on these degrees of freedom. It may be an impossible goal.

3. In principle, QCD gives a complete description of the nucleon and all its excited states. In the simple quark model, the nucleon moment arises from the quark spins, and the first excited state arises from a spin-isospin-flip transition of a quark. Nevertheless, even within QCD, some part of the internal properties of the baryon and its excited states, particularly at large distances, must be equivalent to the strong interaction of hadrons discussed above.

The Relationship Between QHD and QCD

There is now considerable evidence that quantum chromodynamics (QCD), based on quarks and gluons as the underlying degrees of freedom, is the theory of the strong interaction. The colored quarks and gluons are confined to the interior of the hadrons by the strong nonlinear gluon couplings in QCD. At low momenta or large distances,

(o)The *isoscalar* anomalous moment vanishes in this approximation; experimentally it is indeed very small.

(p)This is reminiscent of the *bootstrap* theory of hadronic structure; all hadronic resonances were to be viewed as arising dynamically from the interactions of these same hadrons.

the renormalized coupling constant is large, and QCD is a strong-coupling field theory; in this domain, the observed degrees of freedom are the hadrons. At large momenta, or short distances, QCD is asymptotically free, which implies that the renormalized coupling constant is small; here one can do perturbation theory with free quarks and gluons.

What is the relationship of QHD, the subject of this paper, and the underlying theory of QCD? There are several possibilities:

1. There is an approximate radius R in the hadron outside of which one can use QHD to describe the strong-interaction structure and inside of which one can use quarks and (asymptotically free) QCD. This is the basis of *bag models* of hadrons.[100]

2. One can attempt a similar separation in momentum space. The contribution of the nearby (low-mass) singularities in the spectral representations can be computed from hadronic processes, and the distant contributions can be computed from asymptotically free QCD. The two contributions can then be joined in some manner. This is the basic concept of QCD sum rules.[101]

3. One can assume two models for two different phases of nuclear matter: a baryon/meson phase described by QHD, and a quark/gluon phase described by (asymptotically free) QCD. The two descriptions can be connected with the thermodynamic conditions for phase equilibrium, as discussed earlier in this paper. The investigation of the phase diagram of nuclear matter with the Relativistic Heavy Ion Collider (RHIC) is a top priority for nuclear physics.

More generally, it is probable that at low energies and large distances, QCD can be represented by an *effective field theory* formulated in terms of a few hadronic degrees of freedom. This has indeed been shown to hold in the large-color limit of QCD. In QED, LePage has shown how to construct such a low-energy, large-distance effective field theory.[102] The couping constants in the effective lagrangian are computed from the short-distance behavior of the full, renormalized theory of QED. All possible couplings must be included in the low-energy effective lagrangian, which is then to be used at the "tree level" (that is, without considering loop integrals).

The underlying assumption of QHD is that of a local, relativistic quantum field theory formulated in terms of baryons and the lightest mesons $(\sigma, \omega, \pi, \rho)$. It is assumed that the theory is *renormalizable*, and one then attempts to extract predictions for long-range phenomena by computing both tree-level diagrams *and* renormalized quantum loop corrections. In the end, it may turn out that this assumption is unwarranted, and that the only meaningful interpretation of QHD is as an *effective* theory, to be used at the tree (or one-loop) level. The limitation to renormalizable couplings may then be too restrictive. Nevertheless, the phenomenological success of the MFT of QHD-I in the nuclear domain implies that *whatever the effective field theory for low-energy, large-distance QCD, it must be dominated by linear, isoscalar, scalar and vector interactions.* Recent calculations based on QCD sum rules indicate that this may indeed be true,

as they find evidence for large (several hundred MeV) contributions to the scalar and vector parts of the baryon self-energy in nuclear matter.[103]

SUMMARY AND OUTLOOK

This paper is concerned with the theory of relativistic, interacting, nuclear many-body systems (baryon number $B \geq 1$). The only consistent theoretical framework for describing such systems is relativistic quantum field theory based on a local lagrangian density. As in nonrelativistic many-body theory, Feynman rules for the Green's functions allow one to calculate physical observables.

In this work we argue that the most efficient degrees of freedom for extrapolating away from the observed properties of nuclei are the hadrons: baryons and mesons. We require that the theory be renormalizable (*quantum hadrodynamics*); this defines a self-consistent, *purely* hadronic theory and severely constrains the form of the interaction. We focus on simple models: QHD–I, which contains neutrons, protons and the isoscalar, Lorentz scalar and vector (σ,ω) mesons; and QHD–II, the extension to include the isovector π and ρ mesons based on the linear sigma model.

The development starts with the relativistic mean-field (MFT) and Hartree approximations to QHD–I, and their application to both infinite nuclear matter and atomic nuclei. The principal new feature of the relativistic theory is that the baryon self-energy contains large Lorentz scalar and vector pieces, whose effects cancel in the binding energy but add in the spin-orbit interaction. We present some successes of the model, including the nuclear equation of state, the shell model, nucleon–nucleus scattering, and the addition of zero-point vacuum corrections.

We then discuss extensions to include quantum-loop processes, such as the contribution of two-nucleon correlations to the ground-state energy, the relativistic random-phase approximation for nuclear excitations, and two-loop contributions to the correlation energy. We discuss under what situations the MFT is stable against the inclusion of these effects (that is, when the MFT results are qualitatively unchanged) and when it is not. We also examine issues raised by the role of the quantum vacuum in QHD.

Pions are included within the framework of the chiral-invariant sigma model with spontaneously broken chiral symmetry (QHD–II). It is argued that the scalar field of QHD–I is to be associated with the low-mass dynamical enhancement in the $(0^+,0)$ channel produced by the strong pion couplings, and *not* with the *chiral* scalar field, which may in fact be very massive. It is also shown that the first excited state of the nucleon, the $\Delta(1232)$, which plays such an important role in intermediate-energy nuclear physics, arises dynamically in QHD–II through the summation of nucleon exchange graphs—the relativistic extension of Chew–Low theory.

There is now convincing evidence that *quantum chromodynamics* based on quarks and gluons as the underlying degrees of freedom is the actual theory of the strong interaction; however, the derivation of nuclear structure from the strong-coupling, nonlinear,

confining QCD lagrangian is far in the future.[q] We discuss the relationship between QHD and QCD. Possibilities include: an approximate separation in coordinate space for hadrons, with an exterior region where one uses QHD and an interior region where QCD is used; a separation in momentum space, where QHD is used for nearby singularities and QCD for those far away (QCD sum rules); and an interpretation in terms of two models for two distinct phases of nuclear matter.

More generally, it is probable that at low energies and large distances, QCD can be represented by an *effective field theory* formulated in terms of a few hadronic degrees of freedom. All possible couplings must be included in the low-energy effective lagrangian, which is then to be used at tree level. The underlying assumption of QHD is that of a local relativistic theory formulated in terms of baryons and the lightest mesons. The theory is assumed to be renormalizable, and one then attempts to extract predictions for long-range phenomena by computing both tree-level diagrams *and renormalized quantum loop corrections.* In the end, it may turn out that this assumption is untenable, and that the only meaningful interpretation of QHD is as an *effective* theory, to be used at the tree or one-loop level. The limitation to renormalizable couplings may then be too restrictive. Nevertheless, the phenomenological success of the MFT of QHD–I in the nuclear domain implies that *whatever the effective field theory for low-energy, large-distance QCD, it must be dominated by linear, isoscalar, scalar and vector interactions.*

What is the outlook? Future work will focus on problems such as:

- The investigation of meson propagation and the behavior of the dynamically induced hadronic resonances in nuclear matter.
- The theoretical search for other dynamically induced resonances.
- The study of the modification of nucleon properties in the nuclear medium. This includes the study of the nucleon–meson vertex functions in QHD.
- The continued attempt to solve QHD–II, including σ, ω, π, and ρ, as a strong-coupling field theory.
- The demonstration that QCD leads to large isoscalar, Lorentz scalar and vector interactions between baryons. (There is already some evidence from QCD sum rules that this is the case.)
- A continued effort to describe the internal structure of hadrons and the phase transition to the quark-gluon plasma through strong-coupling, lattice-gauge-theory simulations of QCD.
- Experimental studies of the behavior of nuclear systems under extreme conditions, which challenge our understanding of the nucleus, through new facilities such as the Continuous Electron Beam Accelerator Facility (CEBAF) and the Relativistic Heavy Ion Collider (RHIC).

[q] In this regard, contemplate deriving superconductivity or superfluidity directly from the lagrangian of *quantum electrodynamics.*

This work was supported in part by the US Department of Energy.

REFERENCES

1. B. D. Keister and R. B. Wiringa, Phys. Lett. **173B**, 5 (1986).
2. D. Gogny, in: *Nuclear Physics with Electromagnetic Interactions* (H. Arenhövel and D. Drechsel, eds.), Lecture Notes in Physics, vol. 108, p. 88, Springer, Berlin (1979).
3. J. M. Eisenberg and W. Greiner, *Nuclear Theory*, vols. I–III, North-Holland, Amsterdam (1987).
4. J. A. McNeil, J. R. Shepard, and S. J. Wallace, Phys. Rev. Lett. **50**, 1439 (1983).
5. J. R. Shepard, J. A. McNeil, and S. J. Wallace, Phys. Rev. Lett. **50**, 1443 (1983).
6. B. C. Clark, S. Hama, R. L. Mercer, L. Ray, and B. D. Serot, Phys. Rev. Lett. **50**, 1644 (1983).
7. B. D. Serot and J. D. Walecka, Adv. Nucl. Phys. **16**, 1 (1986).
8. G. Baym and L. P. Kadanoff, Phys. Rev. **124**, 287 (1961).
9. G. Baym, Phys. Rev. **127**, 1391 (1962).
10. E. Dagotto, A. Moreau, and U. Wolff, Phys. Rev. Lett. **57**, 1292 (1986).
11. F. Karsch, Nucl. Phys. **A461**, 305c (1987).
12. R. J. Furnstahl, R. J. Perry, and B. D. Serot, Phys. Rev. C **40**, 321 (1989).
13. W. E. Caswell and A. D. Kennedy, Phys. Rev. D **25**, 392 (1982).
14. J. C. Collins, *Renormalization*, Cambridge University Press, New York (1984).
15. R. Machleidt, K. Holinde, and Ch. Elster, Phys. Rep. **149**, 1 (1987).
16. R. Machleidt, Adv. Nucl. Phys. **19**, 189 (1989).
17. R. Vinh Mau, in: *Mesons in Nuclei*, vol. I (M. Rho and D. H. Wilkinson, eds.), North-Holland, Amsterdam (1979), p. 151.
18. P. G. Reinhard, Rep. Prog. Phys. **52**, 439 (1989).
19. J. D. Walecka, Ann. Phys. (N.Y.) **83**, 491 (1974).
20. B. D. Serot, Phys. Lett. **86B**, 146 (1979); **87B**, 403(E) (1979).
21. T. Matsui and B. D. Serot, Ann. Phys. (N.Y.) **144**, 107 (1982).
22. J. Schwinger, Ann. Phys. (N.Y.) **2**, 407 (1957).
23. M. Gell-Mann and M. Lévy, Nuovo Cim. **16**, 705 (1960).

24. B. Lee, *Chiral Dynamics*, Gordon and Breach, New York (1972).

25. J. D. Bjorken and S. D. Drell, *Relativistic Quantum Mechanics*, McGraw-Hill, New York (1964).

26. J. D. Bjorken and S. D. Drell, *Relativistic Quantum Fields*, McGraw-Hill, New York (1965).

27. C. Nash, *Relativistic Quantum Fields*, Academic, New York (1978).

28. C. Itzykson and J. Zuber, *Quantum Field Theory*, McGraw-Hill, New York (1980).

29. P. Ramond, *Field Theory: A Modern Primer*, Benjamin, Reading, MA (1981).

30. J. I. Kapusta, *Finite-Temperature Field Theory*, Cambridge University Press, New York (1989).

31. D. G. Boulware, Ann. Phys. (N.Y.) **56**, 140 (1970).

32. R. A. Freedman, Ph. D. thesis, Stanford University, 1978.

33. C. W. Misner, K. S. Thorne, and J. A. Wheeler, *Gravitation*, Freeman, San Francisco (1973).

34. Ya. B. Zel'dovich, Sov. Phys. JETP **14**, 1143 (1962).

35. A. R. Edmonds, *Angular Momentum in Quantum Mechanics*, 2nd. ed., Princeton University Press, Princeton, NJ (1957).

36. C. J. Horowitz and B. D. Serot, Nucl. Phys. **A368**, 503 (1981).

37. E. S. Abers and B. W. Lee, Phys. Rep. **9C**, 1 (1973).

38. J. W. Negele, Phys. Rev. C **1**, 1260 (1970); private communication (1982).

39. I. Sick and J. S. McCarthy, Nucl. Phys. **A150**, 631 (1970).

40. B. Frois, J. B. Bellicard, J. M. Cavedon, M. Huet, P. Leconte, P. Ludeau, A. Nakada, Phan Xuan Hô, and I. Sick, Phys. Rev. Lett. **38**, 152 (1977).

41. I. Sick, J. B. Bellicard, J. M. Cavedon, B. Frois, M. Huet, P. Leconte, P. X. Hô, and S. Platchkov, Phys. Lett. **88B**, 245 (1979).

42. J. Boguta, Nucl. Phys. **A372**, 386 (1981).

43. A. Bohr and B. Mottelson, *Nuclear Structure*, vol. I, Benjamin, New York (1969).

44. L. Ray and P. E. Hodgson, Phys. Rev. C **20**, 2403 (1979).

45. W. H. Furry, Phys. Rev. **50**, 784 (1936).

46. L. D. Miller, Phys. Rev. C **9**, 537 (1974).

47. L. D. Miller, Phys. Rev. C **12**, 710 (1975).

48. A. L. Fetter and J. D. Walecka, *Quantum Theory of Many-Particle Systems*, McGraw-Hill, New York (1971).

49. C. E. Price and G. E. Walker, Phys. Rev. C **36**, 354 (1987).

50. S.-J. Lee, J. Fink, A. B. Balantekin, M. R. Strayer, A. S. Umar, P.-G. Reinhard, J. A. Maruhn, and W. Greiner, Phys. Rev. Lett. **57**, 2916 (1986); **59**, 1171(E) (1987); **60**, 163 (1988).

51. W. Pannert, P. Ring, and J. Boguta, Phys. Rev. Lett. **59**, 2420 (1988).

52. R. J. Furnstahl, C. E. Price, and G. E. Walker, Phys. Rev. C **36**, 2590 (1987).

53. G. Leander and S. E. Larsson, Nucl. Phys. **A239**, 93 (1975).

54. D. Vautherin, Phys. Rev. C **7**, 296 (1973).

55. J. A. McNeil, L. Ray, and S. J. Wallace, Phys. Rev. C **27**, 2123 (1983).

56. L. Ray, Phys. Rev. C **19**, 1855 (1979).

57. S. A. Chin, Ann. Phys. (N.Y.) **108**, 301 (1977).

58. R. J. Furnstahl, Ph. D. thesis, Stanford University, 1985; Phys. Lett. **152B**, 313 (1985).

59. P. Blunden and P. McCorquodale, Phys. Rev. C **38**, 1861 (1988).

60. J. R. Shepard, R. Rost, and J. A. McNeil, Phys. Rev. C **40**, 2320 (1989).

61. J. F. Dawson and R. J. Furnstahl, Phys. Rev. C **42**, 2009 (1990).

62. R. J. Furnstahl, in: *Relativistic Nuclear Many-Body Physics* (B. C. Clark, R. J. Perry, and J. P. Vary, eds.), World Scientific, Singapore (1989), p. 337.

63. G. Leibbrandt, Rev. Mod. Phys. **47**, 849 (1975).

64. C. J. Horowitz and B. D. Serot, Phys. Lett. **140B**, 181 (1984).

65. R. J. Perry, Phys. Lett. **182B**, 269 (1986).

66. D. A. Wasson, Phys. Lett. **210B**, 41 (1988).

67. R. J. Furnstahl and C. E. Price, Phys. Rev. C **40**, 1398 (1989).

68. W. R. Fox, Nucl. Phys. **A495**, 463 (1989).

69. P. G. Blunden, Phys. Rev. C **41**, 1851 (1990).

70. K. Huang, *Quarks, Leptons, and Gauge Fields*, World Scientific, Singapore (1982).

71. R. J. Rivers, *Path Integral Methods in Quantum Field Theory*, Cambridge University Press, New York (1987).

72. S. Gottlieb, Nucl. Phys. **B20** (Proc. Suppl.), 247 (1991).

73. R. J. Furnstahl and B. D. Serot, Phys. Rev. C **43**, 105 (1991).

74. G. Baym and S. A. Chin, Phys. Lett. **62B**, 241 (1976).

75. E. Braaten and R. D. Pisarski, Phys. Rev. Lett. **64**, 1338 (1990); Nucl. Phys. **B337**, 569 (1990).

76. R. D. Pisarski, Nucl. Phys. **A525**, 175c (1991).

77. B. D. Serot, in: *From Fundamental Fields to Nuclear Phenomena* (J. A. McNeil and C. E. Price, eds.), World Scientific, Singapore (1991), p. 144.

78. C. J. Horowitz and B. D. Serot, Nucl. Phys. **A399**, 529 (1983).

79. A. F. Bielajew and B. D. Serot, Ann. Phys. (N.Y.) **156**, 215 (1984).

80. C. J. Horowitz and B. D. Serot, Phys. Lett. **B137**, 287 (1984); Nucl. Phys. **A464**, 613 (1987); Nucl. Phys. **A473**, 760(E) (1987).

81. M. R. Anastasio, L. S. Celenza, W. S. Pong, and C. M. Shakin, Phys. Rep. **C100**, 327 (1983).

82. R. Brockmann and R. Machleidt, Phys. Lett. **B149**, 283 (1984); Phys. Rev. C **42**, 1965 (1990).

83. R. J. Furnstahl, Phys. Rev. C **38**, 370 (1988).

84. R. J. Furnstahl and C. J. Horowitz, Nucl. Phys. **A485**, 632 (1988).

85. R. J. Perry, Phys. Lett. **B199**, 489 (1987).

86. T. D. Cohen, M. K. Banerjee, and C.-Y. Ren, Phys. Rev. C **36**, 1653 (1987).

87. C. J. Horowitz and J. Piekarewicz, Phys. Rev. Lett. **62**, 391 (1989); Nucl. Phys. **A511**, 461 (1990).

88. H. Kurasawa and T. Suzuki, Nucl. Phys. **A490**, 571 (1988).

89. K. Wehrberger and F. Beck, Nucl. Phys. **A491**, 587 (1989).

90. X. Ji, Phys. Lett. **B219**, 143 (1989).

91. K. Lim, Ph. D. thesis, Indiana University, 1990.

92. R. J. Furnstahl and B. D. Serot, Nucl. Phys. **A468**, 539 (1987).

93. K. Wehrberger, R. Wittman, and B. D. Serot, Phys. Rev. C **42**, 2680 (1990).

94. J. Milana, Phys. Rev. C **44**, 527 (1991).

95. S. Weinberg, Phys. Rev. Lett. **18**, 188 (1967); Phys. Rev. **166**, 1568 (1968); Physica **A96**, 327 (1979).

96. J. F. Dawson and J. Piekarewicz, Phys. Rev. C **43**, 2631 (1991).

97. A. K. Kerman and L. D. Miller, in: *Second High-Energy Heavy Ion Summer Study*, Lawrence Berkeley Laboratory report LBL–3675 (1974).

98. W. Lin and B. D. Serot, Phys. Lett. **B233**, 23 (1989); Nucl. Phys. **A512**, 637 (1990).

99. W. Lin and B. D. Serot, Nucl. Phys. **A524**, 601 (1991).

100. R. K. Bhaduri, *Models of the Nucleon—From Quarks to Solitons*, Addison-Wesley, Reading, MA (1988).

101. A. Radyushkin, *Lectures on QCD Sum Rules*, CEBAF, Newport News, VA (1991), to be published.

102. P. LePage, in: *From Fundamental Fields to Nuclear Phenomena* (J. A. McNeil and C. E. Price, eds.), World Scientific, Singapore (1991), p. 117.

103. T. D. Cohen, R. J. Furnstahl, and D. K. Griegel, Phys. Rev. Lett. (1991), in press.